Arabian Journal of Chemistry (2023) **16**, 104443

King Saud University

Arabian Journal of Chemistry

www.ksu.edu.sa
www.sciencedirect.com

ORIGINAL ARTICLE

Isotherm modelling and optimization of oil layer removal from surface water by organic acid activated plantain peels fiber

Benjamin Nnamdi Ekwueme [a], Chinonso Anthony Ezema [b,c], Christian O. Asadu [d,*], Chijioke Elijah Onu [e], Thomas O. Onah [f], Innocent Sunday Ike [g,h], Anselem Chinonyelum Orga [g]

[a] *Department of Civil Engineering, Faculty of Engineering, University of Nigeria, Nsukka, Enugu State, Nigeria*
[b] *Department of Microbiology, University of Nigeria, Nsukka, Enugu State, Nigeria*
[c] *Graduate School of Life Science, Hokkaido University, 060-0810 Sapporo, Japan*
[d] *Department of Chemical Engineering, Gregory University P.M.B 1012, Uturu, Abia State, Nigeria*
[e] *Department of Chemical Engineering, Nnamdi Azikiwe University, Awka, Nigeria*
[f] *Department of Mechanical Engineering, Enugu State University of Science and Technology, Enugu, Nigeria*
[g] *Deaprtment of Chemical Engineering, Federal University of Technology, Owerri, Imo State, Nigeria*
[h] *African Centre of Excellence in Future Energies and Electrochemical System (ACE-FUELS), Federal University of Technology, Owerri, Nigeria*

Received 6 January 2022; accepted 17 November 2022
Available online 25 November 2022

KEYWORDS

Esterification;
Thermodynamics;
Response surface methodology;
Artificial neural network;
Langmuir' isotherm

Abstract This research aimed to optimize and model the adsorption process of oil layer removal using activated plantain peels fiber (PPF), a biomass-based material. The adsorbent was activated by thermal and esterification methods using human and environmentally friendly organic acid. Effects of process parameters were examined by one factor at a time (OFAT) batch adsorption studies, revealing optimal conditions for oil removal. Also, RSM, ANN and ANFIS were used to adequately predict the oil removal with correlation coefficient > 0.98. RSM modelling revealed the best conditions as 90 °C, 0.2 mg/l, 1.5 g, 6 and 75 mins, for temperature, oil–water ratio, adsorbent dosage, pH and contact time respectively. Under these simulated conditions, the predicted oil removal was 96.88 %, which was experimentally validated as 97.44 %. Thermodynamic studies revealed the activation energy, change in enthalpy and change in entropy for irreversible pseudo-first order and pseudo-second order model as (15.82, 24.17, −0.614 KJ/mols) and (33.21,40.31,

* Corresponding author.
E-mail addresses: aasadu@yahoo.com, a.christian@gregoryuniversityuturu.edu.ng (C.O. Asadu).
Peer review under responsibility of King Saud University.

Production and hosting by Elsevier

https://doi.org/10.1016/j.arabjc.2022.104443

Nomenclature

EDX	Energy dispersive X-ray spectrometer
XRD	X-ray diffraction
RSM	Response Surface Methodology
CCD	Central Composite Design
PPF	Plantain peel fiber
AAN	Artificial Neural Network
ANFIS	Adaptive network-based fuzzy inference system
SEM	Scanning Electron Microscope
FTIR	Fourier Transform Infrared Spectroscope
ANOVA	Analysis of Variance

−0.106 KJ/mols) respectively, indicating non-spontaneous process; while modeling studies revealed that the adsorption process was highly matched to Langmuir's isotherm, with maximum adsorption capacity of 50.34 mg/g. At the end of the overall statistical modelling, ANFIS performed marginally better than the ANN and RSM. It can be concluded from these results that our biomass-based material is an efficient, economically viable and sustainable adsorbent for oil removal, and has potentials for commercialization since the process of adsorption highly matched with standard models, and its capacity or percentage oil removal also compares favorably to that of commercially available adsorbents.

1. Introduction

Food shortage in OPEC countries, e.g., Nigeria, is imminent if the level of oil devastation of the environment, especially water bodies, is not handled as soon as possible, as oil spillages inhibits agricultural activities (Banerjee et al., 2012). Nigerian Bureau of Statistics in her 2020 report stated that the volume of oil spill in Nigeria is unquantifiable due to lack of accurate data (Reza et al., 2013). Green environment has, over the years, eluded the oil-producing Niger Delta region of Nigeria, and this was caused by the effect of oil pollution (Banerjee et al., 2012; Reza et al., 2013; Annunciado et al., 2005). Oxygen depletion in water bodies due to oil spills have made it difficult to sustain oceanic fauna in this part of the world (Annunciado et al., 2005; Behnood et al., 2013). Causes of this spillage have been traced to oil exploration, tanker accidents, underground pipe breakdown, etcetera (Banerjee et al., 2012; Kharoune et al., 2001; Gwendoline, 2010).

Different approaches to tackling this pollution crisis have been investigated, such as chemical remediation (Muhammed et al., 2019a; Muhammed et al., 2019b), bioremediation (Kharoune et al., 2001; Kumar, 2006; Ladhe et al., 2011; Nwabanne et al., 2018; Thompson et al., 2020), as well as other innovations on wastewater treatment such as coagulation (Suidan et al., 2005; Ayotamuno et al., 2006; Yang et al., 2006). All these methods do not seem to be financially feasible (Banerjee et al., 2012; Baars, 2002) which has prompted further research on adsorption techniques, which have been generally adjudged to be a viable alternative because the process is easier to approach than others. Also, it gives room for the application of ordinary bio-waste thereby reducing the operating cost since the adsorbents are locally synthesized (Reza et al., 2013; Abd et al., 2022; El Bestawy et al., 2020; Abd El-Monaem et al., 2022; Omer et al., 2021).

Conventional adsorbents (e.g sol gel, zeolite, etc) are very costly and are not always available. This has necessitated calls for an immediate search for viable alternatives. The use of agro-industrial wastes for clean technology (e.g., adsorption of contaminants) is actually gaining attention due to its simplicity, low cost, effectiveness, biodegradability and reusability (Ogbodo et al., 2021; Asadu et al., 2021). Among these biowastes, plantain and banana-derived wastes have been reported to be highly efficient for the uptake of various kind of pollutants even in their natural form (Onwu et al., 2019; Asadu et al., 2018). More so, plantain and banana are fruits that are grown all over the world, generating huge volume of fibers that are rich in cellulose, lignin, and hemicellulose-materials with potentials as adsorbents (Annunciado et al., 2005).

Researchers have recently synthesized adsorbents using agro-industrial wastes such as groundnut shell (Banerjee et al., 2012), wood (Albert et al., 2016), kola nut shell (Chinonye et al., 2018), banana peels (Ogbodo et al., 2021; Ekpete et al., 2017), plantain pseudo stem fiber (Asadu et al., 2022), etcetera, but there are variations in the methods of biomass activation, with some methods using mineral acids and alkalis (Chinonye et al., 2018) posing additional risks to the environment. This is one of the shortcomings this present work intends to address by using stearic acid, a human and environmentally friendly organic acid, for activation of the biomass.

Moreover, there has been a limited number of published works on use of plantain peel fiber as adsorbent for crude oil removal. Plantain-derived fibers have been investigated by other researchers as potential raw materials for the production of many materials, e.g., fiber board (Alvarez-López et al., 2014), but its potential as adsorbents have not been extensively studied. It is therefore very important to close the aforementioned gap by synthesizing alternative adsorbent from plantain peels fiber.

To this effect, this current study intends to (i) explore the possibility of synthesizing adsorbent suitable for the remediation of oil polluted water using plantain peel fiber (ii) investigate the thermodynamic characteristics of the process using non-parametric isotherm models; as well as (iii) optimize the efficiency-determining parameters using RSM, ANN and ANFIS.

Chemical thermodynamics studies, among others, the role of entropy, enthalpy and free energy in the process of chemical reactions or diffusion of molecules (Chinonye et al., 2018; Egbuna et al., 2019), while optimization is a way of genuinely generating the best output under certain conditions according to Asadu et al. (Asadu et al., 2019). The use of artificial intelligence models has been reported to greatly enhance many industrial processes unlike the one factor at a time (OFAT). Some of the models such as Adaptive network-based fuzzy inference system (ANFIS), artificial neural network (ANN) and response surface methodology (RSM) have reportedly been used in modeling of many industrial processes with significant success (Onwu et al., 2019; Egbuna et al., 2019; Nnaemeka et al., 2021;

Ezenwa et al., 2019; Ugwele et al., 2020). While there have been some reports on oil removal as already highlighted, no reported work has considered the comparative use of these artificial intelligence models to simulate and optimize the removal of oil from polluted water via an adsorption unto modified plantain peel wastes.

2. Materials and method

2.1. Sample collection pretreatments and preparation

Plantain peels used in this work were sampled from Genesis Restaurant within Enugu metropolis, Enugu State, Nigeria. Unripped plantain peels was sliced into smaller pieces, cleaned using deionized water, then dried under intense sun for seven days and oven dried at 110 °C for 5 h. It was thereafter reduced to fine powder with grinder and sieved to particle size of 75 μm, and was designated as raw PPF. Stearic acid, sulphuric acid (H_2SO_4), Hydrochloric acid (HCl) and caustic soda (NaOH) used in this work were purchased from major market in Enugu Nigeria. The reagents have a purity of 99.9 % and were applied without any treatment or purification. The crude oil used in this work was sourced from Agip oil field Bayelsa State Nigeria.

2.2. Carbonization of PPF and activation with stearic acid

The approaches of Nick et al. (Ogbodo et al., 2021) and Christian et al. (Asadu et al., 2021) were adopted with little modification. The oven dried sample of raw PPF was subjected to thermal treatment in a muffle furnace (model HCK 15/4 No: 20–40509, Taiwan) at 700 °C for 4 h. PPF after heat treatment was allowed to cool down to room temperature and allowed standing for further 45 mins. Then 15 g of the carbonized samples were added to a Dean Stark apparatus and treated with 0.8 g of stearic acid in 200 ml of 100 % *n*-hexane which also contain 1 % H_2SO_4 as catalyst. Refluxing of the mixture at 68 ± 1 °C was done for 2.5 h, followed by washing with distilled water followed by *n*-hexane to remove excess acid. The samples were later dried in oven again at 100 °C for 7 h and stored in a tight polyethylene container. Changes in the weight of the sample were evaluated using equation (1).

$$Percentage\ change\ in\ weight = \frac{Increase\quad in\quad weight}{Initial\quad weight} \times 100 \tag{1}$$

2.3. Physical properties and instrumental characterization

The physical properties of the PPF (raw, carbonized and esterified) were determined according to the standard procedures described by Association of Official Analytical Chemists (Didem, 2012; Cadena et al., 2017). The properties include volatile matter, iodine number, ash content, fixed carbon, moisture content, etc. (Table 3). Bulk density was determined via water displacement method. The BET surface area and its properties were determined using nitrogen gas method. The adsorption–desorption isotherms were calculated at 77 K with assumed nitrogen surface area of 0.162 nm^2 (Ogbodo et al., 2021). The instrumental analysis was done via Scanning Electron Microscope (SEM) (JOEL JSM 6400 model) and Fourier Transform Infrared (FTIR) spectrophotometer (Shimadzu FTIR-8400S). The surface morphology of both the raw PPF and esterified PPF were determined using the SEM while the functional groups present in the samples were identified via FTIR. Elemental composition was determined with an energy dispersive X-ray spectroscopy (EDX, Oxford X-max) coupled to the SEM.

2.4. General experimental procedure for oil layer removal by PPF (raw, carbonized or esterified)

This experiment was conducted following the method described by Nick et al. (Ogbodo et al., 2021) and Banergee et al. (Banerjee et al., 2006). Briefly, 50 ml of 50 mg/l of crude oil–water mixture was produced by mixing known amount of crude oil and water for 10 mins at room temperature, in a 200 ml beaker. With the crude oil floating on surface of water, 0.2 g of the prepared PPF (raw, carbonized or esterified) were added and the mixture agitated for 3 min at 100 rpm. The pH of the mix was adjusted to 7 using 0.1 M NaOH or 0.1 M HCl, and the system incubated at 30 °C for 60 min, before removal of the adsorbent using 50 μm sieving net. The oil-loaded adsorbents (PPF) were dried at 65 °C for 35 min and re-weighed. The experiment was then repeated with oil water concentration of 100 mg/l, 150 mg/l, 200 mg/l and 250 mg/l. Temperature, pH, adsorbent dosage, as well as contact time were also varied to determine their effects. Amount of oil removed was obtained from weight after adsorption and pre-weight of the PPF (raw, carbonized or esterified). Equation (2) (Cheenmatchaya and Kungwakunakorn, 2014) was applied in determining the capacity of adsorption (qe) while the percentage oil removal was determined using equation (3).

$$\text{Adsorption capacity(qe)} = \frac{(Co - Ce)}{M} V \tag{2}$$

$$\text{Percentage of oil removed} = \frac{(Co - Ce)}{Co} \times 100 \tag{3}$$

Where;

C_o = Initial oil concentration (mg/l).

C_e = Concentration oil in oil–water mixture at equilibrium (mg/l).

V = Volume of the oil–water mixture (ml).

M = Mass of the adsorbent (raw, carbonized or esterified PPF).

2.5. Isotherm modeling of the oil layer removal using esterified PPF

To predict the model that best explains the process of crude oil adsorption onto esterified PPF in experiment 2.5, some of the selected models as listed in Table 1 were examined.

2.6. Thermodynamics and activation energy studies of the process using PPF

Thermodynamics investigation was done to estimate the enthalpy (ΔH), entropy (ΔS), and Gibb's free energy of activation (ΔG) for the sorption of oil onto the pores. These thermodynamic properties are vital ingredients for interpreting the behavior of adsorption process (Nwabanne et al., 2018; Asadu et al., 2021). To calculate these parameters, activation complex theory established by Eyring was used in evaluating

Table 1 Selected isotherm models investigated.

Model	Equation	Equation number	Reference
Langmuir	$\frac{C_e}{q_m}=\frac{1}{bq_m}+\frac{C_e}{q_m}$ *and* $R_L=\frac{1}{[1+bC_o]}$	(4)	(Paulauskiene., 2019)
Dubinin Radushkevich	$\mathrm{In}q_e = \mathrm{In}\ q_n\text{-}\beta_e^2\varepsilon = \mathrm{RTIn}\ (1+1/C_e)$	(5)	(Nestor et al., 2004)
Freundlich	$logq_e = \mathrm{i/n}logc_e + logK_f$	(6)	(Asadu et al., 2021)
Temkin	$q_e = \frac{RT}{bT}\mathrm{ln\ A} + \frac{RT}{bT}lnC_e$	(7)	(Olufemi et al., 2014)
Elovich	$In\frac{q_e}{C_e} = InK_eq_m - \frac{q_e}{q_m}$	(8)	(Thompson et al., 2020)

the thermodynamic parameters from temperature-dependent rate constants. Parameters calculated from the Eyring-Polanyi equation (9) are analogous to the Arrhenius equation:

$$k=\frac{k_BT}{h}exp\left(-\frac{\Delta G}{RT}\right) \tag{9}$$

Natural logarithm of equation (9) taken and substituting the value of $\Delta G=\Delta H-T\Delta S$ gives equation (10):

$$In\left(\frac{k}{T}\right)=-\frac{\Delta H}{R}\left(\frac{1}{T}\right)+\left[In\left(\frac{k_B}{h}\right)+\frac{\Delta S}{R}\right] \tag{10}$$

K is the rate constant at temperature T, ΔH and ΔS are the changes in enthalpy and entropy of activation for the reaction system, respectively. k_B and h are the Boltzmann (1.38 X 10^{-23} J K^{-1}) and Planck (6.63 X 10^{-34} Js) constants while R stands for the universal gas constant. Equation (9) is analogous to Van't Hoff equation explaining the mathematical connection existing between enthalpy and entropy of activation with the rate constant. The plot of $In(k/T)vs\frac{1}{T}$ gave the slope as $-\Delta H/R$ and intercept as $[In(k_B/h)+\Delta S/R]$, respectively. Furthermore, the energy of activation is the energy level of the molecules needed to initiate a reaction or diffusion of molecules onto the microporous surface of the PPF. In a second order model, rate constants increase with temperature and is described by the Arrhenius law as shown in equation (11).

$$K=A\exp\left(\frac{-E_a}{RT}\right) \tag{11}$$

Where: K = stands for adsorption rate constant (L g^{-1} min^{-1}).

A = stands for temperature independent factor (L $g^{-1}min^{-1}$).

E_a = stands energy of activation (J mol^{-1}).

R = stands for gas constant (8.314 J mol^{-1} K^{-1}).

T = stands for absolute suspension temperature (K).

When equation (11) is linearized, equation (12) is obtained. From the plot of Ln (K) verses I/T, the values of the Activation energy (E_a) and the temperature independent factor (A) were obtained from the slope and the intercept of the plot, respectively.

$$\mathrm{In(K)} = \mathrm{In\,(A)} + \left(\frac{-\mathrm{E_a}}{\mathrm{R}}\right)\frac{1}{\mathrm{T}} \tag{12}$$

2.7. Central composite design (CCD) and optimization

Central composite design of response surface methodology (CCD-RSM) was used in the experimental design. It consists of five coded levels of lower axial, low, medium, high, and upper axial points, denoted by -α, −1, 0, +1, and + α, respectively. An alpha value of 1.633 was used to account for the design orthogonality. An empirical second-order polynomial expressed in equation (13) was appropriate in describing the effect of the input parameters and their interactions on the percentage of crude oil removed.

$$Y(\%) = \beta_o + \sum\beta_iX_i + \sum\beta_{ii}X_i^2 + \sum\beta_{ij}X_iX_j + \ldots + e \tag{13}$$

Where Y is the percentage of crude oil removed, β_o is the second-order model constant, β_i, represent the coefficient of the first-order term, β_{ii}, is the coefficient of the second-order term, β_{ij} is the coefficient of the interaction between any two variables; e is the random error (Ogbodo et al., 2021). Fisher's test (F-test) and Correlation coefficient (R^2) were used to evaluate the significance and the ranking of the models. Confidence level of 95 % was used in the analysis. The independent parameters examined were temperature X_1(°C), oil concentration X_2(mg/l), adsorbent dosage X_3(g), pH X4, and time X_5 (mins). These parameters were the independent factors whereas the percentage of oil adsorbed or removed (%R) was the dependent parameter or response. The ranges of time, temperature, dosage, oil concentration in water and pH of the adsorption reaction mixture were 15 to 75 mins, 20 to 100 °C, 0.3 to 1.5 g, 0.2 to 1.0 mg/l and 2 to 10, respectively were selected. The coded and uncoded levels of these independent variables are shown in Table 2.

2.8. ANN modelling

Artificial neural network (ANN) was used to model the oil removal process. It is usually viewed as a synchronous process which processes information by the neural system with high accuracy (Chijioke Elijah Onu, 2022a; Onu et al., 2022). The neural toolbox of MATLAB version 8.5.0 was utilized in the ANN modeling with Levenberg-Marquardt back propagation as the training algorithm. It functions via a gradient descent optimization technique (Xuedan et al., 2017). The ANN network consists of input layer, hidden layer and output layer. The input layer consists of five neurons depicting the five input variables while the output layer consists of one neuron representing the output variable. The transfer functions used in the input, hidden and output layers were linear, tansigmoid and purelin transfer functions respectively.

To reduce scaling effect, the data points were normalized between 0 and 1 according to equation (13).

$$x^l=\left(\frac{x_i-x_{min}}{x_{max}-x_{min}}\right) \tag{14}$$

Table 2 Uncoded and coded levels of independent variables.

Variable	Symbol	Axial (-α)	Low	Center	High	Axial (+α)
Level		−2	−1	0	1	2
Temperature (°C)	X_1	0.0	20	60	100	140
Oil Concentration (g/100 cm^3)	X_2	0.0	0.2	0.6	1.0	1.4
Adsorbent dosage (g)	X_3	0.0	0.3	0.9	1.5	2.1
pH	X_4	0.0	2	6	10	14
Time (mins)	X_5	0.0	15	45	75	105

Table 3 BET surface area and physical properties of raw PPF, carbonized PPF and esterified PPF.

Property	Raw PPF	Carbonized PPF	Esterified PPF
Multipoint BET surface area (m^2/s)	10.88	234.51	503.26
Average pore width (nm)	3.22	4.77	7.208
Micropore volume (cm^2/g)	0.008	0.018	0.194
Adsorption energy (KJ/mol)	3.142	3.163	3.885
Pore radius (Å)	8.12	10.18	17.14
Bulk density (g/ml)	0.081	0.101	0.541
pH	8.1	7.54	6.6
Ash content (%)	10.12	8.77	4.08
Iodine Number (mg/g)	326.11	283.1	261.33
Moisture content (%)	11.75	3.84	3.33
Porosity (η)	0.131	0.148	0.891
Volatile matter (%)	47.3	29.66	26.82
Fixed Carbon (%)	31.22	57.73	65.58

Where X_i, X_{max}, and X_{min} are the original data, maximum data, and minimum data for each input and output respectively. X^1 is the normalized value of X_i. (Rekhate and Shrivastava, 2020).

The number of neurons in the hidden layer directly affects the performance of the neural network. Hence the number of neurons in the hidden layer was used in determining the best network performance by comparing the experimental data with the model's responses. Iteration method was used to obtain the optimum number of neurons in the hidden layer. The data division was done such that 80 % of the data was used in training, 10 % was used for testing while the remaining 10 % was used for validation of the network.

2.9. ANFIS modeling

Fuzzy Logic toolbox of MATLAB version 8.5.0 was used in the ANFIS modeling as a hybrid of fuzzy and neural networks. The ANFIS architecture is made up of five layers which represent fuzzification, multiplication, normalization, defuzzification, and summation functions sequentially (Onu et al., 2022). Sugeno fuzzy inference system (FIS) was used to convert the process variables into membership values via the membership functions (MF). Each process variables were assigned to five MF from the input layer. The input layer denoted the five process variables (adsorbent dosage, temperature, contact time, oil concentration and pH) while the output layer denoted the output response (percentage of oil removal). The data set was divided into 80 %, 10 % and 10 % for training, testing, and validation/checking respectively.

2.10. Assessment of the model's performance

Statistical indices were used to assess and rank the performance of the models. The statistical indices used were correlation coefficient (R^2), mean relative percent deviation (MRPD), hybrid fractional error (HYBRID), root mean square error (RMSE) and normalized standard deviation (Δq) as shown in equations 15–19. The performance ranking was based on higher values of R^2 and low values of HYBRID, RMSE, Δq, and MRPD.

$$R^2 = \frac{\sum_{i=1}^{N}\left(Y_{\mathrm{pred(i)}} - Y_{exp,ave}\right)^2}{\sum_{i=1}^{N}\left(Y_{pred(i)} - Y_{exp,ave}\right)^2 + \sum_{i=1}^{N}\left(Y_{pred(i)} - Y_{\mathrm{exp}(i)}\right)^2} \quad (15)$$

$$Normalizedstandarddeviation(\Delta q)\% = 100x\sqrt{\sum\left(1 - \frac{Y_{pred}}{Y_{exp}}\right)^2} \quad (16)$$

$$MRPD = \frac{100}{N}\sum\left|\frac{Y_{pred(i)} - Y_{\mathrm{exp}(i)}}{Y_{\mathrm{exp}(i)}}\right| \quad (17)$$

$$HYBRID(\%) = \frac{1}{N-P}\sum\left[\frac{\left(Y_{pred(i)} - Y_{\mathrm{exp}(i)}\right)^2}{Y_{\mathrm{exp}(i)}}\right]100 \quad (18)$$

$$RMSE = \sqrt{\frac{1}{N}\sum_{i=1}^{N}\left(\frac{Y_{\mathrm{pred(i)}} - Y_{\mathrm{exp}(i)}}{Y_{\mathrm{exp}(i)}}\right)^2} \quad (19)$$

Where $Y_{exp\ (i)}$ is the experimental oil percentage removal, $Y_{pred\ (i)}$ was the model predicted oil percentage removal, $Y_{exp,ave}$ was the experimentally determined average oil percentage removal, N was the number of experimental runs while P was the number of parameters.

3. Results and discussion

3.1. Characterization of adsorbent

3.1.1. Instrumental analysis of adsorbent

The appearance of different functional groups on the surface of raw PPF and esterified PPF as depicted by FTIR (Fig. 1a and 1b) is an indication of reaction between the stearic acid and some functional groups on the PPF, leading to the disappearance of old and appearance of new peaks on the spectrum. For the raw PPF, the organic substance with bond OH was observed at 3186.9 cm^{-1}, at the same time C—H was observed

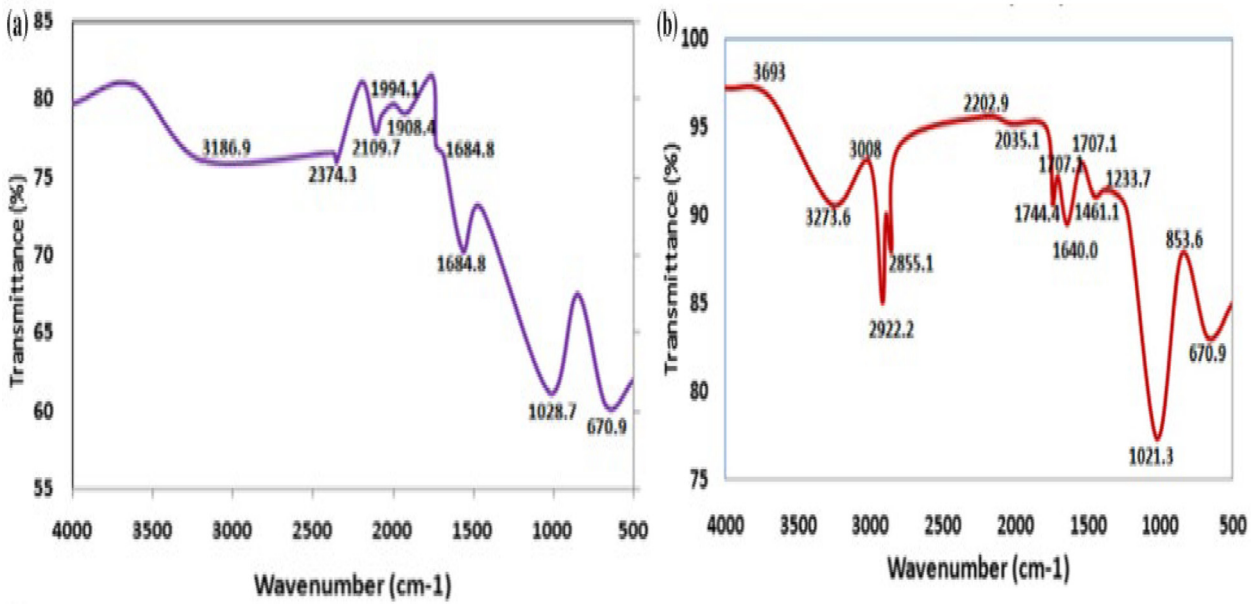

Fig. 1 FTIR spectrum of (a) raw plantain peels and (b) Esterified plantain peels.

at 2374.3 cm^{-1} (Ogbodo et al., 2021). Bands indicating the presence of alkyne were observed between 1908.4 and 2109.7 cm^{-1}. The absorption bands observed at 1684.8 cm^{-1}, 1028.7 cm^{-1} and 670.9 cm^{-1} represents the functional groups C═O, C═C and C─O respectively [42 (Sud et al., 2008). After the modification of the raw plantain peels fiber to esterified PPF, there was a shift in absorption bands as follow; OH, bands were observed between 3273.6 and 3693 cm^{-1}; 2202.9, 2855.3, 2922.3 and 3008 m^{-1} bands represent the alkynes, C═O bands was observed between 1640 and 1744.4 cm^{-1} while C─O bands was observed between 853 and 1021.3 cm^{-1}.

The SEM images depicting the surface morphologies of raw PPF and esterified PPF are shown in Fig. 2 (A and B). Compared to the raw PPF, the esterified PPF displayed a higher number of pores, and hence more potentials as an adsorbent.

X-ray diffraction is widely used to reveal the characteristics of the crystalline structure of substances (Asadu et al., 2021). Shown in Fig. 3a is the XRD spectra of raw PPF and esterified PPF**.** The diffraction pattern of the raw PPF showed the presence of compounds associated to carbon C, iron Fe, aluminon Al and silicon Si. This is evident by diffraction peaks at 2θ values of 27.4°, 41.8°, 53.1°, 57.4°, 65.2° and 71.8°, corresponding to the hexagonal pattern of SiO_2 and $CaCO_3$ as dominant compounds at structural plane 201, 220, 221, 401, 421 and 423, respectively. For the esterified PPF, the appearance of new characteristic diffractions at 2θ values of 31.5°, 36.4°, 44.3°, 52.2°, 59.3°, 66.4° and 77.8° were observed, corresponding to the structural planes of 312, 402, 420, 510, 441 and 445, respectively. The changes in the structural planes could be attributed to the disappearance of some compounds after heat

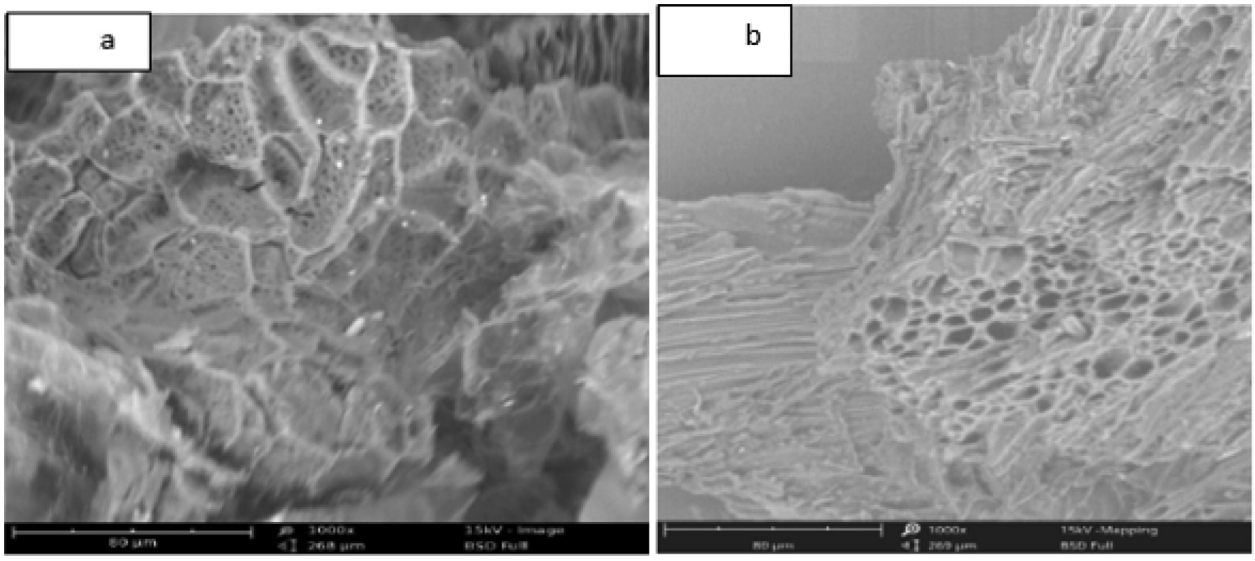

Fig. 2 (a) SEM image of raw PPF at 1000X (b) SEM image of esterified PPF at 1000X.

treatment and impregnation of the carbonized PPF with organic acid giving rise to the hybrid adsorbent. Similar diffraction peaks in other composites have also been reported by Haldorai et al. (Haldorai et al., 2015) and Nsom et al. (Nsom et al., 2019). Nevertheless, the XRD composition of the adsorbents was also supported by the EDX results, as shown in Fig. 3b and 3c. EDX percentage weight compositions of C (57.15), Fe (11.87), Si (11.65), K (10.17) and Al (9.16) were obtained for raw PPF, while C (93.20), Si (2.07), Ca (3.09), and Mg (1.64) were recorded for esterified PPF.

3.1.2. Physical properties of adsorbent

The physical properties of the adsorbents were given in Table 3. The pore properties and surface area of the adsorbents were determined using BET isotherm analysis. The BET surface area (S_{BET}) of the raw PPF was 10.88 m^2/s while the BET surface area (S_{BET}) of esterified PPF was 503.26 m^2/g respectively. The increase in BET surface area as observed was an indication of more active sites within the esterified PPF which will guarantee more uptake of the polluting oil (Nwabanne et al., 2018; Chinonye et al., 2018; Ezenwa et al., 2019). The pore volume increased from 0.008 to 0.194 m^3/g as well as pore diameter from 3.22 to 7.208 nm while the pore radius rose from 8.12 to 17.14 Å. Generally, the improved pore properties will favor the diffusion of more molecules of oil onto the surface of esterified PPF (Onu et al., 2021). The increase in BET surface area can as well be attributed to the disappearance of volatile organics during thermal and acid treatment of the PPF (Asadu et al., 2022; Ike et al., 2022).

Nevertheless, porosity distribution of 0.891 η was noticed within the surface of esterified PPF while the pH reduced from 8.1 (raw PPF) to 6.6 (esterified PPF), indicating increased dominance of the surface by positively charged groups. The moisture content decreased from 11.75 % in raw PPF to 3.33 % in esterified PPF as expected due to loss of water during activation. Also, there was a simultaneous decrease in volatile matter and increase in fixed carbon contents; this might not be unconnected to the disappearance of some inorganic content of the biomass during thermal and acid treatments as proven by the FTIR analysis. This phenomenon is in agreement with the report by Omar. (Omar, 2012).

3.2. Effect of process parameters on crude oil adsorption by PPF

Fig. 4a portrays the impact of pH on oil layer removal by the PPF biomass. It can be stated that optimum oil removal was observed at pH of 5 with esterified PPF recording the most noteworthy percentage as high as 95.3. Interestingly, the rate of oil removal diminished with further increase in pH. This is because of the effect of pH on the net charge on the adsorbent, as well as on the oil surface. In the adsorption reaction mix, a very high pH leads to abstraction of protons from the charged functional groups on the surface of the adsorbent, reducing the net positive charge and the affinity of the adsorbing sites for the negatively charged

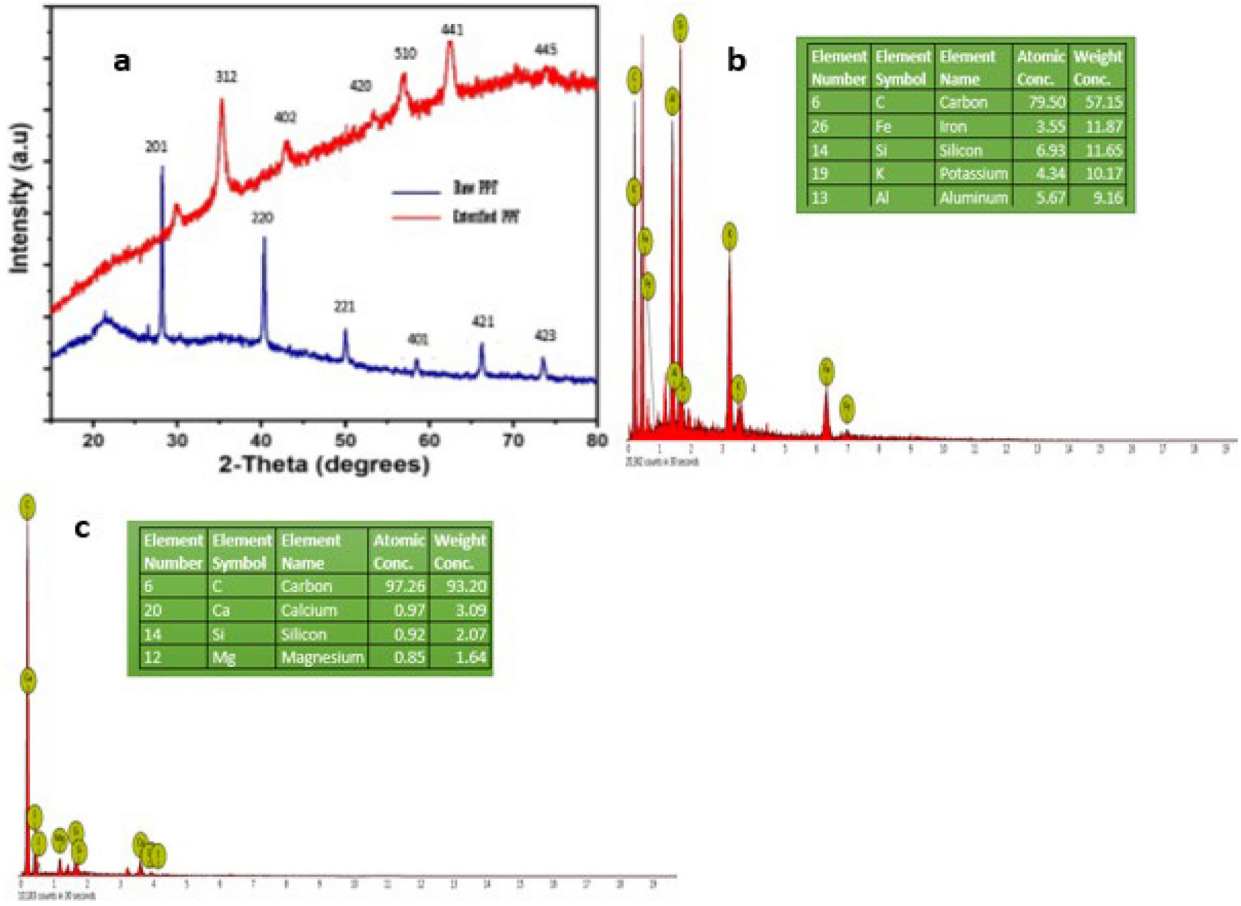

Element Number	Element Symbol	Element Name	Atomic Conc.	Weight Conc.
6	C	Carbon	79.50	57.15
26	Fe	Iron	3.55	11.87
14	Si	Silicon	6.93	11.65
19	K	Potassium	4.34	10.17
13	Al	Aluminum	5.67	9.16

Element Number	Element Symbol	Element Name	Atomic Conc.	Weight Conc.
6	C	Carbon	97.26	93.20
20	Ca	Calcium	0.97	3.09
14	Si	Silicon	0.92	2.07
12	Mg	Magnesium	0.85	1.64

Fig. 3 (a) XRD spectrum of raw PPF and Esterified PPF (a) EDX spectrum of raw PPF (b) EDX spectrum of esterified PPF.

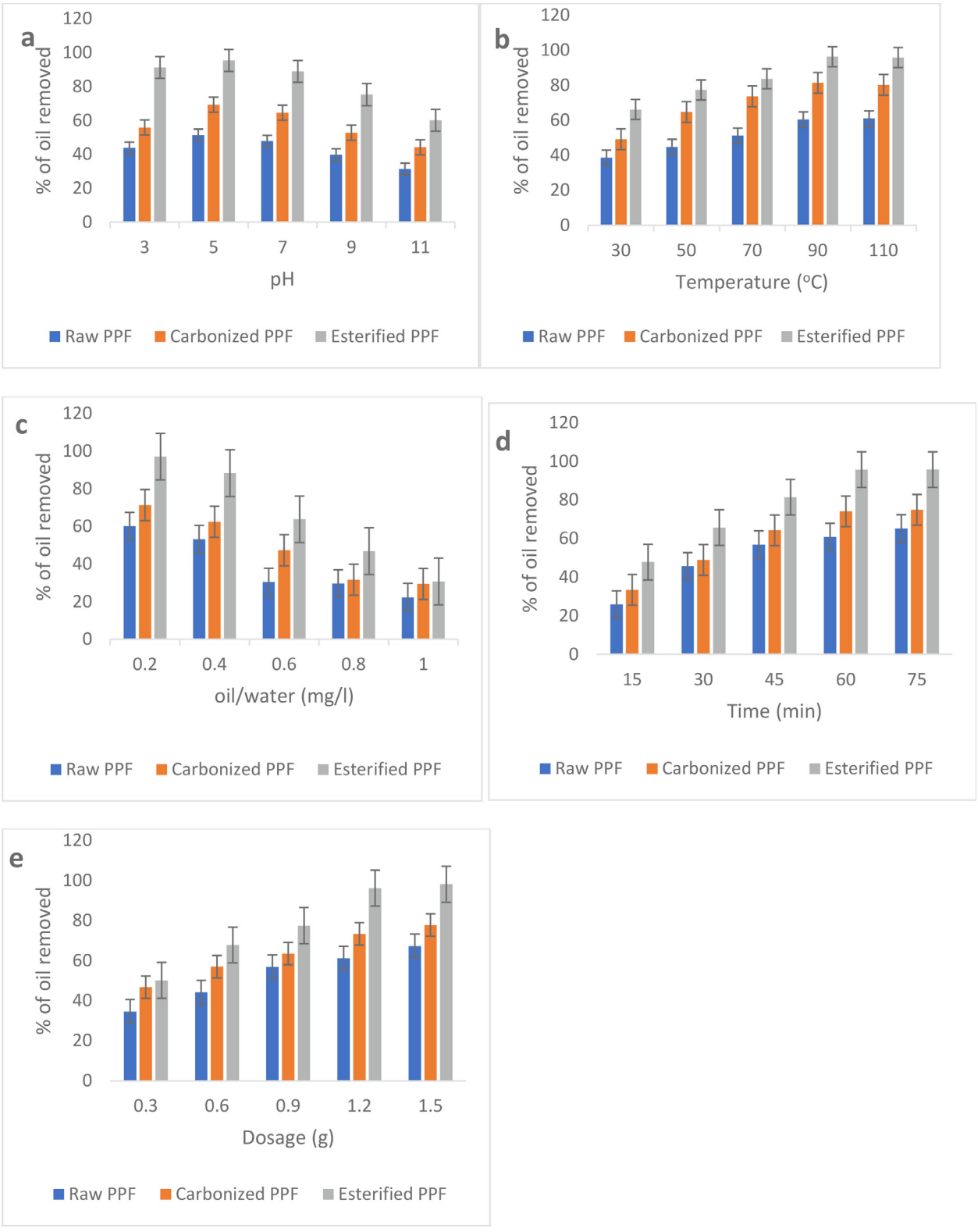

Fig. 4 Effect of pH (a), temperature (b), oil–water ratio (c), time (d), and dosage (e) on crude oil removal by PPF.

oil molecules. This explains why increasing the pH beyond 5 led to successive decrease in the quantity of oil removed (Fig. 4a). A very low pH on the other hand (< 5 in this study), through proton donation, reduces the net negative charge on the oil molecules, also reducing their affinity for the positively charged adsorbent. Similar preference of mild pH range for optimal adsorption of pollutants have also been observed by other researchers (Muhammed et al., 2016; Naema et al., 2014; Ladhe et al., 2011; Pragnesh et al., 2011).

Also, crude oil removal dependency on temperature were evaluated using the developed PPF as depicted in Fig. 4b. It could be seen that crude oil removal by the adsorbents increased with temperature, up until 90 °C. This could be due to improved collision between oil molecules and adsorbents, improved rate of diffusion of oil molecules, or dispersion of oil molecules across the boundary layer and inner pores of the PPF particles. Temperature also changes the interaction of oil molecules, as well as the dissolvability of the oil. Improved rate of pollutants uptake with temperature has also been observed by other researchers (Behnood et al., 2016; Rashmi and Bhattacharya, 2003; Verma and Mishra, 2010; Arivoli et al., 2019).

Moreover, impact of oil–water ratio on oil removal from water surface by PPF was also examined. From Fig. 4c, it is obvious that increasing the ratio, at constant adsorbent dosage, reduces the percentage of oil removed, as the adsorption sites become easily saturated at higher ratio.

Taking from Fig. 4d and Fig. 4e, it can be deduced that increase in contact time and adsorbent dosage increases the amount of oil layers removed which aligns with the general principle of adsorption as stated by Okpe et al. (Chinonye et al., 2018).

Under all the conditions studied, esterified PPF had the best performance, highlighting the efficiency of combined thermal and acid treatments, over thermal treatment alone.

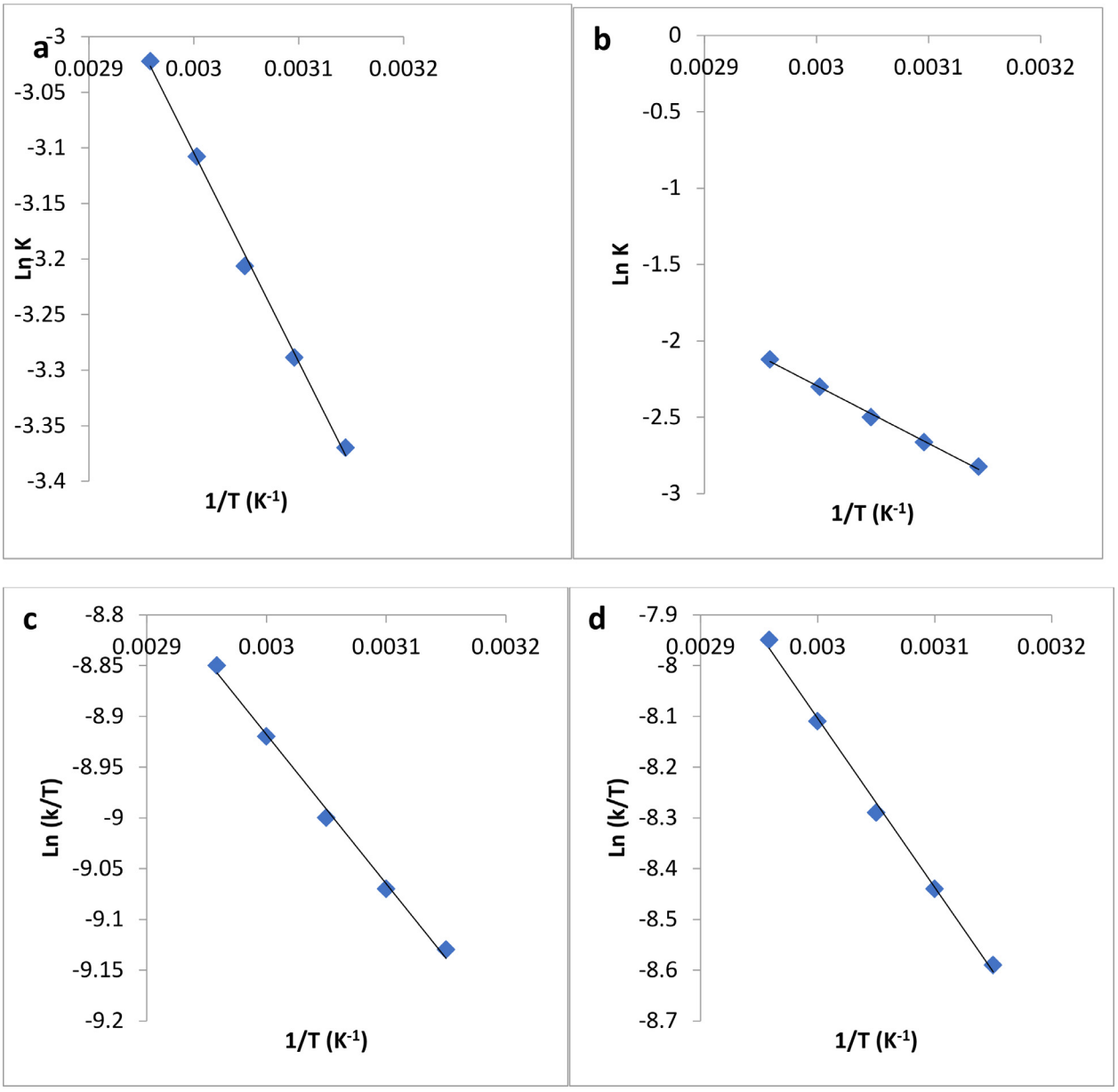

Fig. 5 (a) Plot of In K verses 1/T (K^{-1}) for irreversible pseudo first order model for crude oil sorption by PPF, obtained by using Arrhenius equation. (b) Plot of In K verses 1/T (K^{-1}) for irreversible pseudo second order model for crude oil sorption by PPF, obtained by using Arrhenius equation (c) Plot of Ln (k/T) verses 1/T (K^{-1}) for irreversible pseudo first order model for crude oil sorption by PPF obtained by using Eyring-Polanyi equation (d) Plot of In (k/T) verses 1/T (K^{-1}) for irreversible pseudosecond order model for crude oil sorption onto PPF obtained by using Eyring-Polanyi equation.

3.3. Thermodynamic modeling of the adsorption process

The values of the activation energy, obtained from the slope of the plot of InK verses 1/T (K^{-1}) [see Eqn (9) and Fig. 5a] for the first order model is presented in Table 4 The energy of activation for the diffusion of molecules onto PPF is 15.82 kJ/mol. This value was lower than those given in literature by Chime et al. (Thompson et al., 2020), (53.99 kJ/mol) for the first order for the diffusion of lead ion onto cassava peels adsorbent, although the energy of activation value of PPF sample was within the range reported by Naena et al. (Naema et al., 2014) for lead adsorption using Petiol and Fiber palm tree. Fig. 6.

In the same way, the activation energy values obtained from the slope of the plot of InK against 1/T (K^{-1}) [Eqn (9) and Fig. 5b], for the second order model is also shown in Table 4. The activation energy for PPF sample diffusion is 33.21 kJ/mol. This value was within the range of 38.33 kJ/mol, reported by Okpe et al. (Chinonye et al., 2018) for the second order adsorption of orange G onto kola nut shell. It could be noticed that the Ea value for second order kinetic was higher than that of the first order model. This could be attributed to the higher rate constant value of the pseudo-second order model, when compared to the pseudo-first order model. Behnood et al. (Behnood et al., 2016), also reported similar observation in their work.

Also, Fig. 5c and 5d, show the Eyring plot (Equation (10)) for the sorption and diffusion of oil molecules for irreversible pseudo first and second order models. The values of the thermodynamic parameters (ΔH, ΔS and ΔG) gotten from the plots of 1/T vs In(k/T) (Equation (10) and Fig. 5c) for the pseudo-first order of the studied models is presented in Table 4. Likewise, the thermodynamic parameters (ΔH, ΔS and ΔG) values, for the pseudo-second order model (Equation (10) and Fig. 5d) are also presented in Table 4.

As could be seen in Table 4, the values of ΔH for the irreversible pseudo first order for adsorption of oil onto esterified PPF is 24.17 kJ mol^{-1}. This positive value shows that the energy input from external source is needed to raise the energy level for easy diffusion of oil molecules to the transition state. Hence, indicating that the process is endothermic (Asadu et al., 2021; Asadu et al., 2019). This enthalpy value is similar in range to the 16.35 kJ mol^{-1} obtained for the sorption of oil by spent camellia sinnensis biomass by Falazand and fafique (Fazal and Rafique, 2013). For the entropy change, the value for the irreversible pseudo first order is −0.614 (Table 4).

The negative value suggests the level of associative mechanism that exist, whereby diffusion.

Table 4 Thermodynamics parameters of crude oil sorption by PPF for first and second order models.

T	Irreversible pseudo-first order model				Irreversible pseudo-second order model			
	E_a	ΔH	ΔS	ΔG	E_a	ΔH	ΔS	ΔG
(K)	KJ/mol	KJ/mol	KJ/mol	KJ/mol	KJ/mol	KJ/mol	KJ/mol	KJ/mol
318				13.46				42.30
323				15.23				45.18
328	15.82	24.17	−0.614	17.44	33.21	40.31	−0.106	48.14
333				19.68				50.21
338				20.55				55.24

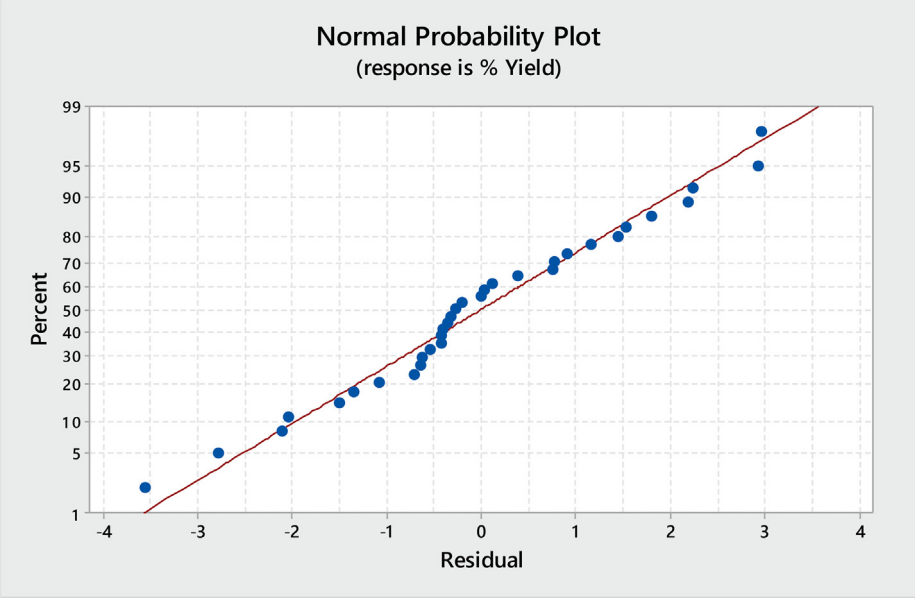

Fig. 6 Normal probability plot of residuals for the removal of crude oil by PPF.

species have combined together to form a more ordered transition state (Asadu et al., 2019; Muhammed et al., 2013). The value is.

within the range given by Muhammed et al, (Muhammed. RabiulAwual et al., 2013) (−0.121 kJ mol^{-1} K^{-1}) and Nick et al. (Onwu et al., 2019);

(−0.18 kJ mol^{-1} K^{-1}) for the sorption of waste cooking and soybean oils, respectively.

The change in Gibb's free energy ΔG value for the irreversible pseudo first order sorption of oil by PPF was found to be in the range of 13.46 – 20.55 kJ mol^{-1} (Table 4). The positive value of ΔG shows the non-spontaneous nature of the process (Nwabanne et al., 2018; Asadu et al., 2021). This obtained value is lower than 88.23 kJ mol^{-1} and 83.30 – 87.69 kJ mol^{-1}, those reported by Ladhe et al. (Ladhe et al., 2011) and Chime et al., (Thompson et al., 2020), for the sorption of waste cooking and lead ion, respectively.

Equally, for the irreversible pseudo second order for adsorption of crude oil onto PPF (Table 4), the ΔH value was 40.31 kJ mol^{-1}. Just like in the pseudo first order model, the positive ΔH shows that there is energy input (heat) from external source necessary to raise the energy level for transformation of reactants to their transition state. Hence, indicating that the process is endothermic (Chinonye et al., 2018). This obtained value of ΔH in the irreversible pseudo second order for adsorption of crude oil onto PPF, was within the range of 28.33 kJ mol^{-1} obtained by Abert et al. (Albert et al., 2016) for the soybean waste adsorbent.

The change in entropy ΔS for the irreversible pseudo second order for crude oil adsorption onto PPF is −0.106 kJ mol^{-1} K^{-1} (Table 4). As earlier stated, this negative value of ΔS, indicates an existence of associative mechanism, whereby reactant combined together to form a more ordered transition state (Asadu et al., 2018). Like in the first order, the obtained value is also within the −0.121 kJ mol^{-1} K^{-1} range reported by Muhammed et al.. (Muhammed et al., 2016) for palm oil adsorption from water.

Finally, the change in free energy ΔG value for the irreversible pseudo second order for crude oil sorption by PPF was found to be in the range of 42.30 – 55.24 kJ mol^{-1} (Table 4). The positive values of ΔG indicate the non-spontaneous nature of the reaction (Egbuna et al., 2019). The value was similar in range to 58.23 kJ mol^{-1} reported by Onwu et al. (Onwu et al., 2019) for crude oil sorption onto groundnut shell.

3.4. Equilibrium or thermodynamic modelling of oil sorption onto PPF

As apparent from the report by (Asadu et al., 2018), adsorption isotherm is the essential prerequisite for planning any sorption framework. It can be said to be a connection between how much a substance eliminated or removed from fluid stage by unit mass of acid treated biomass as sorbent and its amount at constant temperature (Albert et al., 2016; Sheela Tand Arthoba, 2012; Muhammed et al., 2019a). Suitability of the models (see Table 1) was explored and studied. The isotherm boundaries and correlation coefficient (R^2) assessed from the plots of the straight fittings are introduced (see Table 5). R^2 was utilized to anticipate the model with the best fit. The determined dimensionless quantity for the model (see equation 4) called separation factor (R_L) at the four designated temperatures were < 1 (0.2014, 0.0235, 0.1902 and 0.03096) showing ideal sorption. This insight can be attributed to the uniform or homogeneity of circulation or dynamic distribution of active site on the outer layer of the esterified PPF (Asadu et al., 2021). K_f as a constant is a proportion of the adsorption limit while constant n is a proportion of the intensity of the sorption process (Sheela Tand Arthoba, 2012). For beneficial adsorption, the value of n lies somewhere in the range of one to ten (Nwabanne et al., 2018; Muhammed et al., 2013). As it stands in Table 5, it very well may be seen that the value of n at four unique temperature falls somewhere in the range of one to ten (2.645, 1.0956, 3.9056 and 1.8042) uncovering a beneficial sorption for oil layer onto esterified PPF. K_f for equation 6 increases with rise in temperature (see Table 5) showing that adsorption limit of oil onto esterified PPF are leaned toward high temperature. Equation 5 explains that assuming the energy required for activation (E) is under 8 kJ/-mol, the interaction is physisorption, and however assuming the energy of activation is between 8kj/mol and 16 kJ/mol, the cycle is chemisorption in nature (Sud et al., 2008; Muhammed et al., 2013; Kudaybergenov et al., 2015). Additionally, the average free energy of sorption per mole of the adsorbate (Bd) portrays that adsorption is being constrained by particle diffusion mechanism and E > 16 kJ/mol implies an adsorption is represented by molecule dispersion system (Onu et al., 2021; Nwabanne et al., 2017). From Table 5, it is apparent that the energy of activation was below 8kj/mol at each temperature under study showing that the admission of oil from water surface by the esterified PPF is physisorption. Besides, the values for Bd at the selected temperatures studied were under 16 kJ/mol recommending that the sorption of

Table 5 Isotherm parameters evaluated for oil removal by esterified PPF.

Model	Temperature (K)			
	303	323	343	363
Langmuirq				
(mg/g)	51.345	53.129	45.682	10.3349
K_L (L/mg)	1.2490	1.3342	1.4034	1.5201
R_L	0.2014	0.0235	0.1902	0.03096
R^2	0.9910	0.9981	0.9930	0.9990
Dubbin Radushkevich				
B_d	0.002411.324	0.0014828.093	0.03249	0.03345
q_m (mg/g)	0.879	0.9123	56.901	44.975
R^2E	1.0451	2.0957	0.843	0.9012
(kJ/mol)			3.1045	3.1956
Freundlich				
n	2.6145	1.0956	3.9056	1.8042
K_f(L/g)	4.0876	4.9734	6.231	7.357
R^2	0.902	0.7120	0.8023	0.4709
Temkinb				
(J/mol)	4.908	3.0912	2.8057	3.539
K_T (L/g)	1.0743	2.0843	3.0186	4.0896
R^2	0.932	0.9132	0.9067	0.9490
Elovich				
q_m(mg/g)	62.587	80.311	93.400	30.59
Ke	1.3290	1.3098	1.1083	1.790
R^2	0.9160	0.8673	0.9024	0.9610

crude oil onto PPF might not have been controlled by particle diffusion mechanism. In the meantime, the R^2 at each temperature studied as displayed (see Table 5) proposed that the sorption of oil onto esterified PPF might have inclined toward Langmuir isotherm model since the R^2 are nearer to unity than other models at each temperature studied.

3.5. Modeling and variables optimization using RSM, ANN and ANFIS

3.5.1. RSM modelling

Table 2 shows the experimental variables, ranges and level of the independent variables examined in this work using Minitab 17. The percentage of crude oil removed are presented in Table 6. The multiple regression analysis was used for the evaluation of the effects of the independent variables (temperature, dosage, time. amount of oil in mg/1 and pH) on the dependent variable (% of oil removed) (Asadu et al., 2019).

ANOVA test as shown in Table 7 was used to evaluate the statistical significance of the models' equations and the respective model terms. In Table 7, the regression of the intercept, linear, quadratic, and interaction terms of the models use for the adsorption studies were shown. A calculated F value, greater than the F-table (critical F value) value implies that the models were well adequately fitted to the experimental data (Egbuna et al., 2019; Ugwele et al., 2020; Chukwuebuka et al., 2021). Based on a 95 % confidence level, the model were found to be adequate as their respective calculated F values (48.81), were greater than the tabulated $F_{0.05,21,21}$ value of 2.06. Therefore, the terms in the models, ($X_1, X_2, X_3, X_4, X_5, X_1^2, X_2^2, X_3^2, X_4^2, X_5^2, X_1X_3, X_2X_4, X_3X_4$) were all significant. The p-value provides details as to wether a statistical hypothesis is significant or not and how significant it is. When the calculated p-value is less than critical p-value of 0.05, based on 95 % confidence level, the evidence agaist null hypothesis H_0 is stronger (Chinonye et al., 2018; Asadu et al., 2019; Nnaemeka et al., 2021; Ezenwa et al., 2019; Onu et al., 2021). Therefore, the model was found to be significant as the p-value was = 0.000 and < 0.05. Similarly, the terms in the model ($X_1, X_2, X_3, X_4, X_5, X_1^2, X_2^2, X_3^2, X_4^2, X_5^2, X_1X_3, X_2X_4, X_3X_4$) were all significant ($p < 0.05$).

Using Minitab 17.0 software, the full regression model equations' terms and statistical significance were determined. Prior to the removal of the insignificant terms, the second-order polynomial regression models that best described the processes (% of oil removed) as a function of actual values of temperature (X_1), Oil conc (X_2), adsorbent dosage (X_3), pH (X_4) and time (X_5)

Table 6 Experimental design matrix and obtained for the removal of crude oil by esterified PPF.

Run	X_1	X_2	X_3	X_4	X_5	% of oil removed	
						Experimental	Predicted
1	1.000	−1.000	−1.000	−1.000	−1.000	59.61	60.44
2	0.000	0.000	0.000	0.000	0.000	90.48	91.48
3	−1.000	1.000	1.000	−1.000	−1.000	83.09	83.08
4	−1.000	−1.000	1.000	−1.000	−1.000	60.81	60.11
5	1.000	1.000	−1.000	−1.000	1.000	78.88	80.23
6	1.000	−1.000	−1.000	1.000	1.000	78.50	78.51
7	−1.000	−1.000	−1.000	−1.000	1.000	90.67	90.80
8	−1.000	1.000	−1.000	1.000	1.000	78.60	80.10
9	1.000	1.000	−1.000	1.000	−1.000	72.37	77.13
10	−1.000	1.000	−1.000	−1.000	−1.000	60.78	61.03
11	1.000	−1.000	1.000	−1.000	1.000	78.77	79.10
12	0.000	0.000	0.000	0.000	0.000	90.55	90.21
13	−1.000	−1.000	1.000	1.000	1.000	78.80	78.51
14	0.000	0.000	0.000	0.000	0.000	90.60	91.21
15	0.000	0.000	0.000	0.000	0.000	90.65	90.88
16	0.000	0.000	0.000	0.000	0.000	90.77	90.22
17	1.000	1.000	1.000	−1.000	−1.000	70.39	73.18
18	1.000	1.000	1.000	1.000	−1.000	70.49	71.14
19	1.000	−1.000	1.000	1.000	1.000	96.84	96.88
20	−1.000	−1.000	−1.000	1.000	−1.000	60.80	66.45
21	−1.000	1.000	1.000	1.000	−1.000	70.42	71.04
22	0.000	0.000	0.000	0.000	0.000	90.55	93.21
23	0.000	0.000	0.000	0.000	0.000	80.01	83.45
24	0.000	0.000	0.000	−2.000	0.000	62.95	64.23
25	0.000	2.000	0.000	0.000	0.000	73.58	73.55
26	0.000	0.000	−2.000	0.000	0.000	62.85	62.85
27	2.000	0.000	0.000	0.000	0.000	77.11	77.18
28	−2.000	0.000	0.000	0.000	0.000	65.64	66.35
29	0.000	0.000	0.000	2.000	0.000	74.94	75.96
30	0.000	0.000	2.000	0.000	0.000	76.29	76.29
31	0.000	0.000	0.000	0.000	−2.000	55.91	55.93
32	0.000	0.000	0.000	0.000	2.000	81.62	80.64
33	0.000	−2.000	0.000	0.000	0.000	55.48	55.56

Table 7 Analysis of variance (ANOVA) for response surface quadratic models of the studied PPF sample.

Source of Variable	SS	Df	Coeff. (β)	SE coeff.	MS	F-value	P-value
Model (C)	2516.78	21	78.020	0.615	119.847	48.81	0.000
Blocks	132.91	1	0.000	0.606	132.912	49.50	0.000
X_1	180.51	1	2.742	0.334	180.511	67.23	0.000
X_2	338.40	1	3.755	0.334	338.401	126.03	0.000
X_3	248.84	1	3.220	0.334	248.842	92.68	0.000
X_4	197.23	1	2.867	0.334	197.227	73.46	0.000
X_5	923.80	1	6.204	0.334	923.800	344.06	0.000
X_1^2	13.62	1	−1.026	0.298	31.830	11.85	0.005
X_2^2	190.17	1	−2.738	0.298	226.483	84.35	0.000
X_3^2	51.63	1	−1.477	0.298	65.975	24.57	0.000
X_4^2	71.94	1	−1.634	0.298	80.667	30.04	0.000
X_5^2	85.17	1	−1.679	0.298	85.172	31.72	0.000
X_1X_2	8.56	1	−0.731	0.410	8.556	3.19	0.102
X_1X_3	16.28	1	−1.009	0.410	16.281	6.06	0.032
X_1X_4	0.86	1	−0.233	0.410	0.865	0.32	0.582
X_1X_5	0.48	1	0.174	0.410	0.483	0.18	0.680
X_2X_3	6.48	1	−0.636	0.410	6.477	2.41	0.149
X_2X_4	13.40	1	−0.915	0.410	13.396	4.99	0.047
X_2X_5	5.55	1	0.589	0.410	5.546	2.07	0.178
X_3X_4	19.89	1	−1.115	0.410	19.892	7.41	0.020
X_3X_5	11.06	1	0.831	0.410	11.056	4.12	0.067
X_4X_5	0.00	1	−0.010	0.410	0.002	0.00	0.981

[C] Constant.
[SS] Sum of squares.
[Df] Degree of freedom.
[Coeff.] Coefficients.
[SE Coeff.] SE Coefficient.
[MS] Mean square.
X_1: temperature; X_2: oil conc; X_3: dosage.; X_4: pH; X_5: time.
$p < 0.01$ highly significant; $0.01 < p < 0.05$ significant; $p > 0.05$ not significant.
Model Tabulated $F_{0.05,10,10}$ value is 2.06. Hence, $F > 2.06$ significant; $F < 2.06$ insignificant.
Model terms Tabulated $F_{0.05,1,10}$ value is 4.23. Hence, $F > 4.23$ significant; $F < 4.23$ insignificant.

$$
\begin{aligned}
[\%ofoilremoved]_{PPF} &= 89.02 + 2.74X_1 + 3.76X_2 \\
&\quad + 3.22X_3 + 2.87X_4 + 6.20X_5 \\
&\quad - 01.03X_1^2 - 2.74X_2^2 - 1.48X_3^2 \\
&\quad - 1.63X_4^2 - 1.68X_5^2 - 0.73X_1X_2 \\
&\quad - 1.01X_1X_3 - 0.23X_1X_4 \\
&\quad + 0.17X_1X_5 - 0.63X_2X_3 \\
&\quad - 0.92X_2X_4 + 0.59X_2X_5 \\
&\quad - 1.12X_3X_4 + 0.83X_3X_5 \\
&\quad - 0.01X_4X_5 \qquad (20)
\end{aligned}
$$

Similarly, equation (21) show the model equations for the crude oil removal, after all insignificant term have been removed. These insignificant terms are removed based on their p-values in the ANOVA results in Table 7. These removed insignificant terms are those terms whose p-values were > 0.05 (see Table 7).

$$
\begin{aligned}
[\%ofoilremoved]_{PPF} &= 89.02 + 2.74X_1 + 3.76X_2 \\
&\quad + 3.22X_3 + 2.87X_4 + 6.20X_5 \\
&\quad - 01.03X_1^2 - 2.74X_2^2 - 1.48X_3^2 \\
&\quad - 1.63X_4^2 - 1.68X_5^2 - 1.01X_1X_3 \\
&\quad - 0.92X_2X_4 - 1.12X_3X_4 \qquad (21)
\end{aligned}
$$

Table 8 Analysis of variance of regression for response surface.

Regression	R^2 (%)	Adj. R^2 (%)	F-value	P-value
Block	5.22		49.50	0.000
Linear	74.18		140.69	0.000
Quadratic	16.20		30.73	0.000
2-way interaction	3.24		3.07	0.039
Total model	98.88	96.66	48.81	0.000

Table 9 RSM predicted and experimentally validated optimum values for % methyl ester yields.

Sample	% of crude oil removed	
	RSM predicted value	Experimentally validated value
Esterified PPF	96.88	97.44

The characteristics parameters that may express the quality (goodness of fit) of the proposed second order polynomial model (Eqns. 20–21), are the coefficient of determination

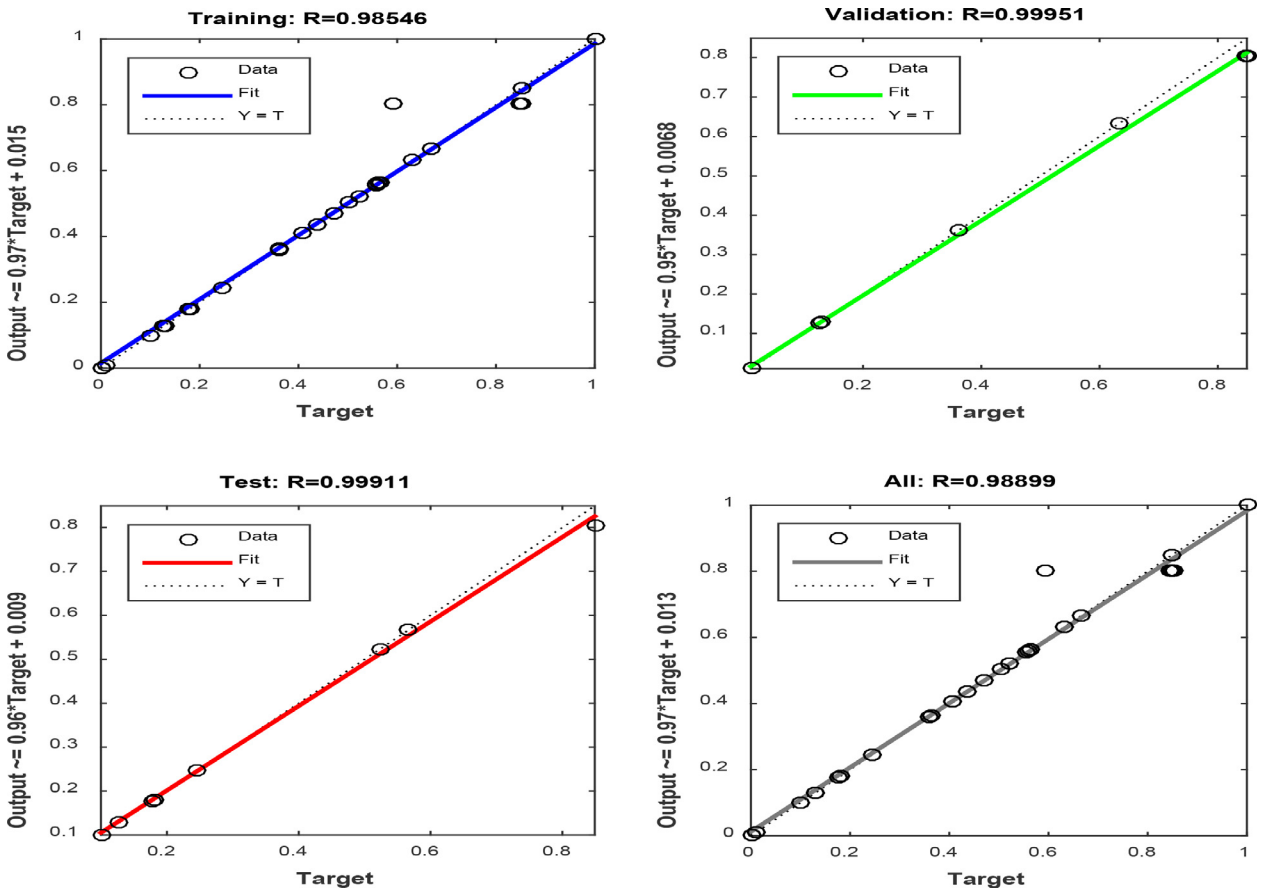

Fig. 7 ANN plots of percentage oil removal using esterified PPF.

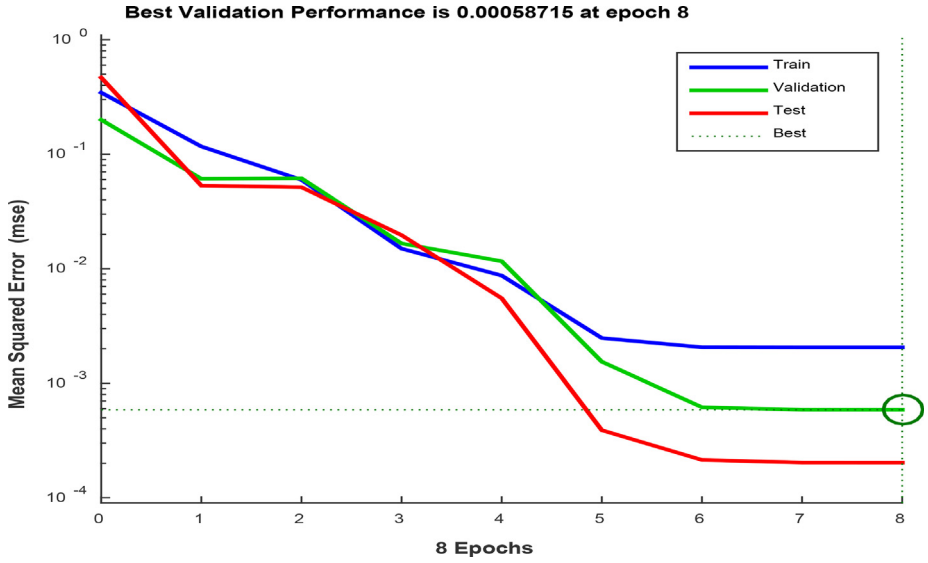

Fig. 8 ANN validation performance plot of the oil removal process.

(R^2) and adjusted R^2 (Adj-R^2) (Ezenwa et al., 2019; Onu et al., 2021). From Table 8, the R^2 value is 98.88. The closer the R^2 to 1 (100 %), the better the fit. Similarly, the R^2 Adj is 96.66. The values of R^2, show significant closeness to 1, hence, indicate good fit. The values of the predicted models R^2 and the Adj-R^2 were both found to be very high. The closeness of predicted models R^2 and Adj-R^2 values, as well as the lower values of Adj-R^2 compared to the R^2 values, for all the models, shows an excellent goodness of data fit (Ogbodo et al., 2021; Asadu et al., 2022). Fig. 6 shows the normal probability plot

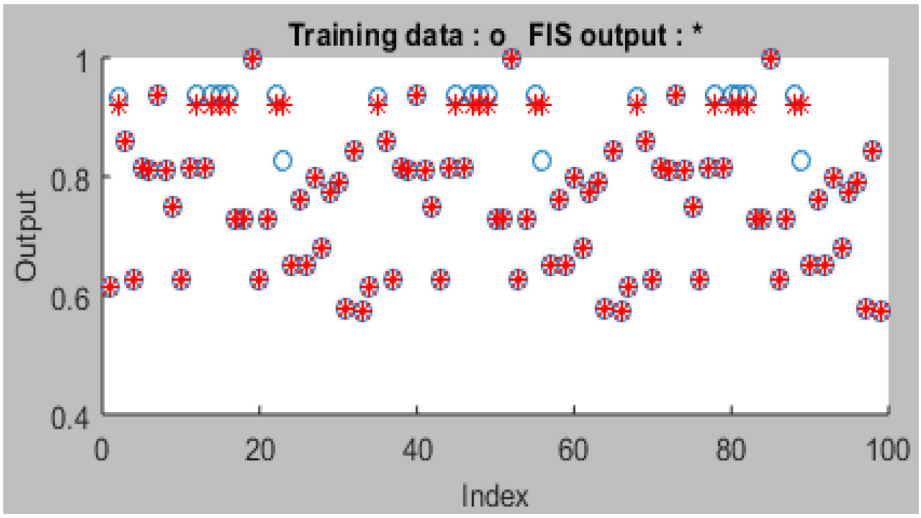

Fig. 9 ANFIS training plot of the percentage oil removal.

for the crude oil removal by PPF. The values of the response predicted from the models are in line with the observed values over the range of the selected operating variables of temperature, oil conc, adsorbent dosage, pH and time.

Table 9 shows the values of the RSM predicted and validated for the adsorption of crude oil by esterified PPF. The optimum conditions for the maximum removal of crude oil samples with respect to the proposed models' equations were 90 °C, 0.2 mg/1, 1.5 g, 6 and 75 mins. At these conditions (Table 9), the predicted value or better still, the theoretical value for the crude oil removal stood at 96.88 %. Also, from Table 9, the experimentally validated value for the percentage crude oil removal was 97.44 %. The validation experiments were done by performing three independent experimental replicates and the average values recorded. The closeness of the validated and predicted oil yields confirmed the competence and validity of the model.

3.5.2. ANN modeling

The analysis of the neural network indicated an optimum of 10 neurons in the hidden layer. This was achieved by varying the neurons in the hidden layer with R^2 and RMSE as the performance index. It was inferred that 10 neurons in the hidden layer will provide the maximum R^2 and minimum RMSE. Therefore, the optimum ANN architecture for the oil removal process has a topology of 5–10-1. This topology gave the best prediction accuracy with minimum deviations. The multi-layer perceptron (MLP) model was used because of its ability in approximating nonlinear processes (Chijioke Elijah Onu, 2022a). The ANN plots of training, testing, and validation in Fig. 7 showed R^2 values of 0.9855, 0.9991 and 0.9995 with RMSE of 2.05×10^{-3}, 5.87×10^{-4}, and 2.03×10^{-4} respectively. The high R^2 values and low RMSE values suggested significant model performance. The testing data set adequately guided against model over-fitting while significant training data set implied that there is a correlated relationship between the input variables and the output response. This was confirmed by the R^2 value of 0.9889 for the overall data.

Furthermore, the neural performance plot (Fig. 8) was used to graphically assert the nature of the neural performance. The figure showed that the training, testing and validation curves stabilized at the 8th epoch iteration with RMSE of 5.87×10^{-4}. The curves attained consistency at the 6th epoch iteration. The nature of the curves suggested adequate neural modeling with no over fitting issues.

Table 10 Statistical analysis of the models.

Statistical Indices	R^2	Δq	HYBRID	RMSE	MRPD
ANN	0.9970	0.0144	0.0422	0.0253	0.64776
ANFIS	0.9982	0.0142	0.0421	0.0209	0.6476
RSM	0.9888	0.1953	0.0479	0.0340	1.3772

3.5.3. ANFIS modeling

The trapezoidal-shaped membership function (*trapmf*) was used to generate the fuzzy inference system (FIS) in the input membership function. Root mean square errors of 0.0067, 0.0032, and 0.0065 were generated for the training, testing, and validation/checking, respectively. Forty-five nonlinear parameters and 243 training pairs and linear parameters were

Table 11 Kinetics parameters of the crude oil adsorption by esterified PPF.

Pseudo first order	
K_1 (min^{-1})	0.00694
q_e (mg/g)	405.23
R^2	0.9990
Pseudo second order	
K_1 (g/mg.min)	0.00123
q_e (mg/g)	300.1
R^2	0.978
Elovich	
β (g/mg)	0.01334
α (g/mg)	2.0963
R^2	0.9850
Lagregan second order	
K_1 (min^{-1})	0.0092
q_e (mg/g)	23.498
R^2	0.9061

Table 12 Relationships in comparison with other works existing in literature.

Adsorbents	Adsorption Capacities (qe) (mg/g)	Equilibrium Time (mins)	Crude oil Concentration (g/100 cm^3)	References
Acetylated Rice Husk	44.8	60	0.3	(Banerjee et al., 2006)
Thermally Activated Rice Husk	46.7	50	0.3	(Kudaybergenov et al., 2015)
Activated Watermelon Waste	28.9	60	0.5	(Banerjee et al., (2012). A)
Commercial Zeolite	55.30	50	0.2	(Naema et al., 2014)
Esterified PPF	50.34	50	0.2	This present study

used for effective ANFIS modeling. Minimum root mean square error of 0.001763 was obtained for the overall data set at 50 epoch iterations with error tolerance of 0.00. Constant membership function was chosen for the output MF while the optimization method used was hybrid. This resulted in ANFIS model with a high R^2 of 0.9982. Fig. 9 showed that the ANFIS predicted oil removal efficiency perfectly tracked the experimental oil removal efficiency as virtually all the ANFIS data points aligned with the experimental data points.

3.5.4. Comparative assessment of the models

The overall performance of the models was assessed using statistical indicators as shown in Table 10. The high R^2 values (>0.98) showed that there is an almost perfect correlation between the models' predicted percentage oil removal and the experimental percentage oil removal. However, the ANFIS performed marginally better than the ANN. The RSM model was the least among the three models. The low values of the error terms (especially HYBRID, RMSE, and Δq) suggested that there were insignificant deviations between from the experimental result.

3.6. Kinetics studies

Pseudo first order, pseudo second order, Elovich's, Lagregan second order models were used to study the time dependency of the crude oil adsorption process. The results of the kinetic analysis, with the correlation coefficients and models' constant were presented in Table 11. Elovich model and pseudo first order model showed good correlation in the kinetic study, however pseudo first order kinetic model best described the kinetics of the crude oil adsorption with R^2 of 0.9990 (Table 11). This implied that chemisorption was the rate-limiting step with presence of valence forces between the crude oil molecules and the adsorbent (Ogbodo et al., 2021; Ugwele et al., 2020). Besides, Elovich's model is usually applied to chemisorption systems with heterogeneous adsorbing surface. The applicability of the pseudo second order inferred a reduction in boundary layer thickness of the PPF at high temperature.

3.7. Comparison between the present studies and prior researches in the similar field

The adsorbent developed from PPF in this work was compared with other adsorbents existing in literature based on performance. The performance was further compared with commercial zeolite adsorbent in the market (see Table 12). The performance index used was the adsorption capacities at a specified period of time. It can be seen that the adsorption capacity of the present study was mostly comparable to the zeolite adsorbent reported by Naena et al., 2014. The most interesting thing about this present study is that we got a relatively high adsorption capacity of 50.34 mg/g at a very short time of 50 mins. The adsorption capacity is far much higher than the ones reported for other agro-wastes (see Table 12). Considering the aforementioned results, we arrived at a conclusion that the PPF used is an efficient low-cost adsorbent for the removal of crude oil from aqueous solution.

4. Conclusion

Plantain peels fiber (PPF) was synthesized via carbonization and esterification processes and used to study the removal of crude oil from surface waste via an adsorption process. The BET surface area analysis indicated that the surface area of the modified adsorbent was significantly increased. Instrumental analysis using FTIR, SEM, XRD and EDX showed that activation with organic acid modified the chemical groups on the PPF. Thermodynamic modelling of the process revealed the activation energy (Ea) for pseudo-first order kinetic modelling and pseudo- second order kinetic modelling as 15.82 and 33.21 KJ/mol while the changes in free energy and enthalpy were positive indicting that the process is non-spontaneous. Isotherm model analysis depicts that the data on the sorption of crude oil onto esterified PPF fitted well with Langmuir isotherm model. ANFIS, ANN and RSM were efficient in modeling the oil removal process but ANFIS performed marginally better than the ANN and RSM. The optimum conditions as predicted by the RSM model was thus: Thus; 90 °C, 0.2 mg/l, 1.5 g, 6 and 75 mins. At this point, the predicted oil removal stood at 96.88 % which was experimentally validated as 97.44 %. The results of this investigation suggested that production of plantain peels fiber adsorbent in commercial quantity to reduce the importation of conventional non-biodegradable and non-environmentally friendly adsorbents is possible. Activation of other bio-wastes through esterification using stearic acid is recommended in order to expand the frontier of achieving green environment through adsorption process.

Declaration of Competing Interest

The authors declare that they have no known competing financial interests or personal relationships that could have appeared to influence the work reported in this paper.

Acknowledgement

The authors wish to appreciate in a special way the Department of Chemical Engineering,

Gregory University Uturu for her numerous contributions and every other person who have.

contributed in one way or the other to the success of this work.

References

Abd El-Monaem, E.M., Omer, A.M., El-Subruiti, G.M. *et al.* (2022), Zero-valent iron supported-lemon derived biochar for ultra-fast adsorption of methylene blue. *Biomass Conv. Bioref.* https://doi.org/10.1007/s13399-022-02362-y.

Eman M.Abd El-Monaem, Abdelazeem S.Eltaweil, Hala M.Elshishini, Mohamed Hosny, Mohamed M.Abou Alsoaud, Nour F.Attia, Gehan M.El-Subruiti, Ahmed M.Omer (2022); Sustainable adsorptive removal of antibiotic residues by chitosan composites: An insight into current developments and future recommendations. *Arabian journal of chemistry* 15(5): 103743 https://doi.org/10.1016/j.arabjc.2022.103743.

Albert, C.A., Asadu, C.O., Onoh, M.I., Azubuike, K.A., 2016. Kinetics and isotherm studieson divalent lead ions adsorption by zeolite solution. Int. J. Novel Res. Eng. Sci. 31, 49–61.

Alvarez-López, C., Rojas, O.J., Rojano, B., Gañán, P., 2014. Development of self-bonded fiberboards from fiber of leaf plantain: effect of water and organic extractives removal. Bio Resour. 10 (1), 672–683. https://doi.org/10.15376/biores.10.1.672-683.

Annunciado, T.R., Sydenstricker, T.H.D., AnucoS, C., 2005. Experimental investigation of various vegetable fibers as sorbent materials for oil spills marine pollution. Bulletin 50, 13040–13046.

Arivoli, S., Hema, M., Martin, P.D., 2019. Adsorption of malachite green onto carbon Prepared from Borassus bark. Arab. J. Sci. Eng. Sect. A Sci. 34 (2A), 31–43.

Asadu, C.O., Egbuna, S.O., Ejikeme, P.C.N., 2018. Survey on kinetic decomposition of organic matter and bio-fertilizer synthesis by composting sawdust, vegetable waste and sewage sludge. J. Chinese Adv. Mater. Soc.

Asadu, C.O., Anthony, E.C., Elijah, O.C., Ike, I.S., Onoghwarite, O. E., Okwudili, U.E., 2021. Development of an adsorbent for the remediation of crude oil polluted water using stearic acid grafted coconut husk (*Cocos nucifera*) composite. Appl. Surf. Sci. Adv. 6, 100179.

Asadu, C.O., Ekwueme, B.N., Onu, C.E., Onah, T.O., Ike, I.S., Ezema, C.A., 2022. Modelling and optimization of crude oil removal from surface water via organic acid functionalized biomass using machine learning approach. Arab. J. Chem. 2022, 104025.

Christian O. Asadu., Samuel O. Egbuna, Thompson O. Chime, Chibuzor N. Eze, DibiaKevin., Gordian O. Mbah Anthony C. Ezema (2019), Survey on solid wastes management by composting: Optimization of key process parameters for biofertilizer synthesis from agro wastes using response surface methodology (RSM). Artificial Intelligence in Agriculture 3, 52–6. https://doi.org/10.1016/j.aiia.2019.12.002.

Christian O. Asadu, O.C. Elijah, N.O. Ogbodo, E.C. Anthony, C.T. Onyejiuwa, M.I. Onoh, I.S. Ike, O.E. Onoghwarite, A.S. Chukwuebuka, (2021a), Treatment of crude oil polluted water using stearic acid grafted mango seed shell (Mangifera indica) composite, Current Research in Green and Sustainable Chemistry 4:100169https://doi.org/10.1016/j.crgsc.2021.100169.

Christian O. Asadu, C.A. Ezema, O.C. Elijah, N.O. Ogbodo, O.I. Maxwell, O.F. Ugwele, A.S. Chukwuebuka, T.O. Onah, E. Godwin-Nwakwasi, I.S. Ike, E.M. Ezeh, (2022, Equilibrium isotherm modelling and optimization of oil layer removal from surface water by organic acid grafted plantain pseudo stem fiber, Case Studies in Chemical and Environmental Engineering), doi: https://doi.org/10.1016/j.cscee.2022.100194.

Asadu, C.O., Onoh, M.I., Albert, C.A., 2018. Equilibrium isotherm studies on the adsorption of malachite green and lead ion from aqueous solution using locally activated Ugwaka Clay (Black Clay). Arch. Curr. Res. Int. 12 (2), 1–11. https://doi.org/10.9734/ACRI/2018/39302. ISSN: 2454-7077.

Ayotamuno, M.J., Kogbara, R.B., Ogafi, S.O.T., Probert, S.D., 2006. Bioremediation of a crude oil polluted agricultural-soil at Port-Harcourt. Nigeria J. Appl. Energy 83, 1249–1257.

Baars, B.J., 2002. The wreckage of the oil tanker 'Erika'-human health risk assessment of beach cleaning, sunbathing and swimming. Toxicol. Lett. 128 (1–3), 55–68.

Banerjee K, Ramesh ST, Gandhimathi R, Nidheesh PV & Bharathi KS (2012).A novel agricultural waste adsorbent, watermelon shell for the removal of copper from aqueous solutions. Iran J Energy Environ 3:143-156.

Banerjee, S.S., Joshi, M.V., Jayaram, R.V., 2006. Treatment of oil spill by sorption technique using fatty acid grafted sawdust. Chemosphere 64, 1026–1031.

Behnood, R., Anvaripour, B., Jaafarzadeh, N., Farasati, M., 2013. Application of natural sorbents in crude oil adsorption. Oil Gas Sci. Technol. J. 2 (4), 01–11.

Behnood, R., Anvaripour, B., Jaafarzadeh, N., Farasati, M., 2016. Oil spill sorption using raw and acetylated sugarcane bagasse. J. Cent. South Univ. 23, 1618–1625. https://doi.org/10.1007/s11771016-3216-8.

Cadena, E.M., Ch, J.M., Vélez, R., Santa, J.F., Viviana, O.G., 2017. Natural fibers from plantain Pseudostem (Musa Paradisiaca) for use in fiber-reinforced composites. J. Nat. Fibers. https://doi.org/10.1080/15440478.2016.1266295.

Cheenmatchaya, A., Kungwakunakorn, S., 2014. Preparation of activated carbon derived from rice husk by simple carbonization and chemical activation for using as gasoline adsorbent. Int. J. Environ. Sci. Develop. 5 (2), 21–33.

Chijioke Elijah Onu, Chinenyenwa Nkeiruka Nweke, Joseph Tagbo Nwabanne (2022a) Modeling of thermo-chemical pretreatment of yam peel substrate for biogas energy production: RSM, ANN, and ANFIS comparative approach. Applied Surface Science Advances 11 (2022) 100299. 1 – 12. https://doi.org/10.1016/j.apsadv.2022.100299

Chinonye, O.E., Oluchukwu, A.C., Elijah, O.C., 2018. Statistical analysis for orange G adsorption using kola nut shell activated carbon. J. Chinese Adv. Mater. Soc. https://doi.org/10.1080/22243682.2018.1534607.

Chukwuebuka, A.S., Samuel, E.O., Asadu, C.O., Onoghwarite, O.E., Celestine, O., Ezema, C.A., 2021. Optimal analysis of the effects of process conditions on the yield of alkyd resins from castor and soybean seed oils using response surface methodology. Chem. Eng. J. Adv. https://doi.org/10.1016/j.ceja.2021.100217.

Didem, O., 2012. An Approach to the Characterization of Biochar and Bio-Oil. Bioengineering Department Yildiz Technical University, Turkey.

Samuel O. Egbuna., Donatus C. Onwubiko.,&Christian O. Asadu (2019a): Comparative Studies and Optimization of the Process Factors for the extraction of Beta-carotene from Palm oil and Soybean oil by Solvent extraction, Journal of Engineering Research and Reports. 8(2): 1-16.

Egbuna, S.O., Onwubiko, D.C., Asadu, C.O., 2019. Kinetics and thermodynamic studies of beta carotene extraction from palm oil by solvent extraction. J. Mater. Sci. Res. Rev. 4 (2), 1–13.

Ekpete, O.A., Marcus, A.C., Osi, V., 2017. Preparation and characterization of activated carbon obtained from plantain (*Musa paradisiaca*) Fruit Stem, Hindawi. J. Chem. 8635615. https://doi.org/10.1155/2017/8635615.

El Bestawy, E., El-Shatby, B.F., Eltaweil, A.S., 2020. Integration between bacterial consortium and magnetite (Fe_3O_4) nanoparticles for the treatment of oily industrial wastewater. World J. Microbiol. Biotechnol. 36 (9), 141. https://doi.org/10.1007/s11274-020-02915-1.

Ezenwa, O., Asadu, C.O., Agaba, A., 2019. Optimization and kinetic modeling of the removal of lead from Enugu coal by acid leaching.

J. Energy Res. Rev. 3 (1), 1–13. https://doi.org/10.9734/jenrr/2019/v3i130090.

Fazal, A., Rafique, U., 2013. Severance of lead by acetylated and esterified *spent camellia sinensis* powder. Am. J. Environ. Eng. 3 (6), 288–296. https://doi.org/10.5923/j.ajee.20130306.04.

Gwendoline, F., 2010. The effects of oil spills of aquatic life and environments. J. Sci. Nat. 2 (4), 23–30.

Haldorai, Y., Kharismadewi, D., Tuma, D., Shim, J.-J., 2015. Properties of chitosan/magnetite nanoparticles composites for efficient dye adsorption and antibacterial agent. Korean J. Chem. Eng. 32, 1688–1693.

Ike, I.S., Asadu, C.O., Ezema, C.A., Onah, T.O., Ogbodo, N.O., Godwin-Nwakwasi, E.U., Onu, C.E., 2022. ANN-GA, ANFIS-GA and thermodynamics base modeling of crude oil removal from surface water using organic acid grafted banana pseudo stem fiber. Appl. Surf. Sci. Adv. 9, 100259.

Kharoune, M., Pauss, A., LebeaultJ, M., 2001. Aerobic biodegradation of an oxygenates mixture: ETBE, MTBE and TAME in an upflow fixed-bed reactor. Water Resour. 35 (7), 1665–1674.

Kudaybergenov, K.K., Ongarbayev, E.K., Mansurov, Z.A., 2015. Oil sorption by heat- treated rice husks. J. Pet. Environ. Biotechnol. 6, 5–13.

Kumar, K.V., 2006. Comparative analysis of linear and non-linear method of estimating the sorption isotherm parameters for malachite green onto activated carbon. J. Hazard. Mater. 136 (2), 197–202.

Ladhe, U.V., Wankhede, S.K., Patil, V.T., Patil, P.R., 2011. Adsorption of eriochromeblackT from aqueous solutions on activated carbon prepared from mosambi peel. J. Appl. Sci. Environ. Sanitation 6 (2), 149–154.

Muhammed. Rabiul Awual.; Md. Munjur Hasan.; Mohammed M. Rahman Abdullah M.Asiri,(2019a)Novel composite material for selective copper(II) detection and removal from aqueous media; Journal of Molecular Liquids, 283:772-780.

Muhammed. Rabiul Awual.;Md. MunjurHasan. Abdullah M.Asiri.; MohammedM.Rahman(2019b): Cleaning the arsenic(V) contaminated water for safe-guarding the public health using novel composite material. Composites Part B: Engineering, 171:294-301.

Muhammed. Rabiul Awual;Md. Munjur Hasan; Gaber E.Eldesoky; Md. AbdulKhaleque; Mohammed M.Rahman; Mu. Naushad (2016),Facile mercury detection and removal from aqueous media involving ligand impregnated conjugate nanomaterials; Chemical Engineering Journal, 290:243-251.

Muhammed.RabiulAwual.;Tohru Kobayashi.;Yuji Miyazaki.; Ryu-heiMotokawa.; Hideaki Shiwaku.; Shinichi Suzuki.; Yoshihiro Okamoto.; Tsuyoshi Yaita;(2013),Selective lanthanide sorption and mechanism using novel hybrid Lewis base (*N*-methyl-*N*-phenyl-1,10-phenanthroline-2-carboxamide) ligand modified adsorbent: Journal of Hazardous Materials, 252-253: 313-320.

Naema A. HikmatBushra B. Qassim, Mohammed T. Khethi (2014), "Thermodynamic and Kinetic Studies of Lead Adsorption from Aquesous Solution onto Petiole and Fiber of Palm Tree"American Journal of Chemistry p-ISSN: 2165-8749 e-ISSN: 2165-8781; 4 (4): 116-124.

Nestor, T., Natalia, M., Fabiana, M., Javier, P., Carina, P., Tomas, C. P., 2004. Adsorption onto powdered and granular activated carbon, prepared from eucalyptus wood. J. Colloid Interface Sci. 279, 357–363.

Nnaemeka, I.C., Samuel, E., Maxwell, O., AsaduChristain, O.C., 2021. Optimization and kinetic studies for enzymatic hydrolysis and fermentation of colocynthis vulgaris Shrad seeds shell for bioethanol production. J. Bioresour. Bioprod. 6, 45–64.

Nsom, M.V., Etape, E.P., Tendo, J.F., Namond, B.V., Chongwain, P. T., Yufanyi, M.D., William, N., 2019. A green and facile approach for synthesis of starch-pectin magnetite nanoparticles and application by removal of Methylene Blue from textile effluent. J. Nanomater. 2019, 1–12.

Nwabanne J.T, Okpe E. C., Asadu C. O. and Onu C.E(2017). Application of Response Surface Methodology in Phenol Red Adsorption Using Kola Nut (*Colaacuminata*) Shell Activated Carbon. International Research Journal of Pure & Applied Chemistry 15(4): 1-14.

Nwabanne, J.T., Okpe, E.C., Asadu, C.O., Onu, C.E., 2018. Sorption studies of dyestuffs on low-cost adsorbent. Asian J. Phys. Chem. Sci. 5 (3), 1–19.

Ogbodo, N.O., Asadu, C.O., Ezema, C.A., Onoh, M.I., Elijah, O.C., InnocentIke, S., Onoghwarite, O.E., 2021. Preparation and Characterization of activated carbon from agricultural waste (Musa-paradisiacapeels) for the remediation of crude oil contaminated water. J. Hazard. Mater. Adv. https://doi.org/10.1016/j.hazadv.2021.100010.

Olufemi, B.A., Jimoda, L.A., Agbodike, N.F., 2014. Adsorption of crude oilusing meshed corncobs. Asian J. Appl. Sci. Eng. 3, 63–75.

Omar, H.A., 2012. Adsorptive removal of phenol from aqueous solution using natural immobilized Chitin by Diathiazone. N. Y. Sci. J. 5 (8), 1–9.

Omer, A.M., Abd, E.M., El-Monaem, G.M., El-Subruiti, M.M., El-Latif, A., Eltaweil, A.S., 2021. Fabrication of easy separable and reusable MIL-125(Ti)/MIL-53(Fe) binary MOF/CNT/Alginate composite microbeads for tetracycline removal from water bodies. Sci. Rep. 11, 23818. https://doi.org/10.1038/s41598-021-03428-z.

Chijioke Elijah Onu, Joseph T. Nwabanne, Paschal E. Ohale, Christian O. Asadu, (2021), Comparative analysis of RSM, ANN and ANFIS and the mechanistic modeling in eriochrome black-T dye adsorption using modified clay,South African Journal of Chemical Engineering 36: :24–42.

Onu, C.E., Ohale, P.E., Obiorah-Okafo, I.A., Asadu, C.O., Okoye, C. C., Ojukwu, E.V., Ezennajiego, E.E., 2022. Application of Rice Husk-Based Biomaterial in Textile Wastewater Treatment. In: Muthu, S.S., Khadir, A. (Eds.), Textile Wastewater Treatment. Sustainable Textiles: Production, Processing, Manufacturing & Chemistry. Springer, Singapore, pp. 231–250. https://doi.org/10.1007/978-981-19-2852-9_12.

Onwu, D. O., O. Nick, O., N. Cordelia, O., O. Asadu, C., & I. Maxwell, O. (2019a). Optimization of Process Parameters for the Treatment of Crude Oil Spill Polluting Water Surface by Sorption Technique Using Fatty Acid Grafted Ogbono Shell as a Sorbent. *Journal of Materials Science Research and Reviews*, *3*(3), 1-12.

Onwu, D.O; Ogbodo, O.N; Ogbodo, N.C; Chime, T.O; Udeh, B.C; Egbuna, S.O; Onoh, MI; Asadu, C.O (2019b) Application of Esterified Ogbono Shell Activated Biomass as an Effective Adsorbent in the Removal of Crude Oil layer from Polluting Water Surface. J. Appl. Sci. Environ. Manage. Vol. 23 (9) 1739-1746.

Paulauskiene, T., Jucike, I., Juseenko, N., Baziuke, D.. The use of natural sorbents For spilled crude oil and diesel cleanup from the water surface.2014.

Pragnesh, N.D., Satindar, K., Ekta, K., 2011. Removal of eriochrome black –T by adsorption onto eucalyptus bark using green technology. Indian J. Chem. Technol. 18, 53–60.

Rashmi, S., Bhattacharya, B., 2003. Adsorption-coagulation for the decolorisation of textile dye solutions. Water Qual. Res. J. Canada 38 (3), 553–562.

Rekhate, C.V., Shrivastava, J.K., 2020. Decolorization of Azo dye solution by ozone based advanced oxidation processes: optimization using response surface methodology and neural network. Ozone Sci. Eng. https://doi.org/10.1080/01919512.2020.1714426.

Reza, B., Bagher, A., Nematollah, J.H.F., Masoumeh, F., 2013. Application of natural sorbents in crude oil absorption. *Iran. J. Oil Gas Sci.* Technol. 2, 01–11.

Sheela Tand Arthoba, N., 2012. Kinetics and thermodynamics of cadmium and lead ions adsorption on NiO nanoparticles. Chem. Eng. J. 191, 123–131.

Sud, D., Mahajan, G., Kaur, M.P., 2008. Agricultural waste material as potential adsorbent for sequestering heavy metal ions from aqueous solutions-a review. Bioreso. Tech. 99, 6017–6027.

Suidan, M.T., Esperanza, M., Zein, P., McCauley, R.C., Brenner, A. D., 2005. Challenges in biodegradation of trace organic contaminants-gasoline oxygenates and sex hormones. Water Environ. Res. 77 (1), 4–11.

Thompson, C.O., Ndukwe, A.O., Asadu, C.O., 2020. Application of activated biomass waste as an adsorbent for the removal of lead (II) ion from wastewater. Emerg. Contamin. 6, 259–267.

Ugwele, F.O., Aninwede, C.S., Chime, T.O., Asadu, C.O., Ike, S.I., 2020. Application of response surface methodology in optimizing the process conditions for the regeneration of used mobil oil using different kinds of acids. Heliyon J., Elsevier Ltd. https://doi.org/10.1016/j.heliyon.2020.e05062.

Verma, V.K., Mishra, A.K., 2010. Kinetic and isotherm modeling of adsorption of dyes Onto rice husk carbon. Global NEST J. 10 (10), 1–7.

Shi Xuedan, Wenqian Ruan, Jiwei Hu, Mingyi Fan, Rensheng Cao and Xionghui We (2017) Optimizing the Removal of Rhodamine B in Aqueous Solutions by Reduced Graphene Oxide-Supported Nanoscale Zerovalent Iron (nZVI/rGO) Using an Artificial Neural Network-Genetic Algorithm (ANN-GA). Nanomaterials 2017, 7, 134; doi:10.3390/nano7060134

Yang, G., Zhang, L., Sun, X., Jing, W., 2006. Photochemical degradation of crude oil in sea water. Chinese J., Oceanol. Limnol. 24 (3), 264–269.